

SwN

DASA 2427

THE ADVANCED DEVELOPMENT OF WATER TRIGATRON
AND THREE-ELECTRODE SULFUR HEXAFLUORIDE SWITCHES

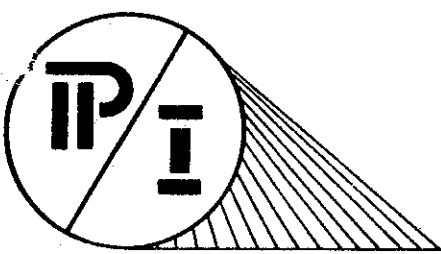
PIFR-114

January 1970

by

T. Fleischman and I. Smith

This research has been sponsored by the
Defense Atomic Support Agency
Under NWER Subtask LA053
Contract DASA-01-68-C-0136

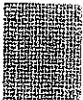


PHYSICS
INTERNATIONAL
COMPANY

3 . 1 4 1 5 9 2 6 5 3 5 8 9 7

2700 Merced St., San Leandro, Calif. 415/357-4610

This document has been
approved for public
release and sale; its
distribution is unlimited.



1
2
3
4
5
6
7
8
9
10
11
12
13
14
15
16
17
18
19
20
21
22
23
24
25

DASA 2427

THE ADVANCED DEVELOPMENT OF WATER TRIGATRON
AND THREE-ELECTRODE SULFUR HEXAFLUORIDE SWITCHES

PIFR-114

January 1970

by

T. Fleischman and I. Smith

This research has been sponsored by the
Defense Atomic Support Agency
Under NWER Subtask LA053
Contract DASA-01-68-C-0136

Physics International Company
2700 Merced Street
San Leandro, California 94577

1
2
3
4
5
6
7
8
9
10
11
12
13
14
15
16
17
18
19
20
21
22
23
24
25
26
27
28
29
30
31
32
33
34
35
36
37
38
39
40
41
42
43
44
45
46
47
48
49
50
51
52
53
54
55
56
57
58
59
60
61
62
63
64
65
66
67
68
69
70
71
72
73
74
75
76
77
78
79
80
81
82
83
84
85
86
87
88
89
90
91
92
93
94
95
96
97
98
99
100

CONTENTS

	<u>Page</u>
I. TRIGATRON SWITCHING IN WATER	1
A. Apparatus	4
B. Experimental Results	16
II. THREE-ELECTRODE, COAXIALLY FED, SF ₆ SWITCH	29
A. Apparatus	32
B. Results	35
III. THREE-ELECTRODE, OPEN TRANSMISSION LINE FED, SF ₆ SWITCH	50
A. Apparatus	50
B. Results	68
IV. EARLY RESISTIVE PHASE MEASUREMENTS	85
A. Risetime Parameters	85
B. Results	86



ILLUSTRATIONS

<u>Figure</u>	<u>Page</u>
1 Water Trigatron	2
2 Water Pulser	5
3 Water Generator Output Voltage Waveform	7
4 Trigatron Firing in Water	8
5 Trigger Pulser Schematic	10
6 Trigger Pulser Assembly	11
7 Trigger Pulser and Coiled Line	13
8 Waveform from Integrated Unshielded B-Loop	15
9 Self-Breakdown Tests	17
10 Trigatron Electrode with Trigger	19
11 Traces Showing Effect of Trigger Pulse on Trigatron	22
12 Typical Experimental Conditions	24
13 Trigatron Experiment Schematic	25
14 Frequency of Triggered and Non-Triggered Delays	26
15 Three-Electrode Field-Enhanced Switch	30
16 Prototype Three-Electrode SF ₆ Switches	33
17 Prototype SF ₆ Switch Firing in Water	34
18 Experiment with Blumlein Trigger	36
19 Self-Breakdown Strength of SF ₆ Switch--dc and Pulsed	38
20 Minimum Trigger Voltage to Fire Either Side of Switch	40
21 Trigger Electrode Waveforms	42

ILLUSTRATIONS (Cont.)

<u>Figure</u>		<u>Page</u>
22	Test Employing an Independent Trigger Source	43 43
23	Average Jitter as a Function of Trigger Voltage and Overall Voltage	46
24	Experimental Circuit	51
25	Three-Electrode SF ₆ Switch (First Configuration)	53
26	Three-Electrode SF ₆ Switch (First Configuration)	54
27	Three-Electrode SF ₆ Switch (Second Configuration)	55
28	Uniform-Field Gap	57
29	I-Gap	58
30	Voltage Traces from Fast CuSO ₄ Monitor	59
31	E-Field Monitor Voltage Trace	61
32	Current Monitor	63
33	S-Gap and M-Gap Voltage Waveforms	64
34	Experimental Circuit Detail	65
35	S-Gap Pressure Versus Breakdown Voltage	69
36	Overall Delay and Jitter of V/3 M-Switch	70
37	Overall Delay and Jitter of V/3 M-Switch	71
38	Overall Delay and Jitter for V/2 M-Switch	75
39	Resistive Phase of Trigger Pulse	87
40	Early Resistive Phase and Voltage Risetime	89

ILLUSTRATIONS (Cont.)

<u>Figure</u>		<u>Page</u>
41	Early Resistive Phase Versus Pressure	90
42	Fraction of Voltage or Current Rise at Which V_{\max} Is Observed	91
43	Risetime of SF ₆ Switch Into 90 Ω	93

0
1
2
3
4
5
6
7
8
9
10
11
12
13
14
15
16
17
18
19
20
21
22
23
24
25
26
27
28
29
30
31
32
33
34
35
36
37
38
39
40
41
42
43
44
45
46
47
48
49
50
51
52
53
54
55
56
57
58
59
60
61
62
63
64
65
66
67
68
69
70
71
72
73
74
75
76
77
78
79
80
81
82
83
84
85
86
87
88
89
90
91
92
93
94
95
96
97
98
99

SECTION I

TRIGATRON SWITCHING IN WATER

A "trigatron" is a switch consisting of three main elements: the two main switch electrodes, the trigger feed point, and the switching medium (Figure 1). The trigger electrode and insulation are contained within one of the main switch electrodes and for convenience the ground electrode is usually chosen. When the trigger pulse is applied it causes local breakdown of the switching medium in the vicinity of the ground electrode which leads subsequently to spark closure between the main electrodes.

Trigatrons in which the switching medium is a gas have been widely used; at Physics International, for example, the multi-megavolt Marx generators which form part of the 730 and 1140 Pulserad facilities are erected by initiating the closure of a single switch (the switch nearest the ground) in this fashion. The use of a trigatron with a liquid switching medium (water in this case) was first reported by Nesterikin in the USSR in 1966. First reports indicated that jitters as low as 5 nsec had been achieved at 300 kV, and the aims of the present study were to demonstrate successful operation of a water trigatron first at 300 kV and then at voltages up to 1 MV.

There are several significant differences between gas and liquid trigatrons. Chief among these is the breakdown process in gases and liquids. In gases, breakdown does not commence until a threshold or breakdown field has been exceeded, when electron avalanche and (usually) fast streamer propagation close the switch in a time of the order of nanoseconds. Thus, a gas trigatron may be dc charged with an electric field close to the breakdown value.

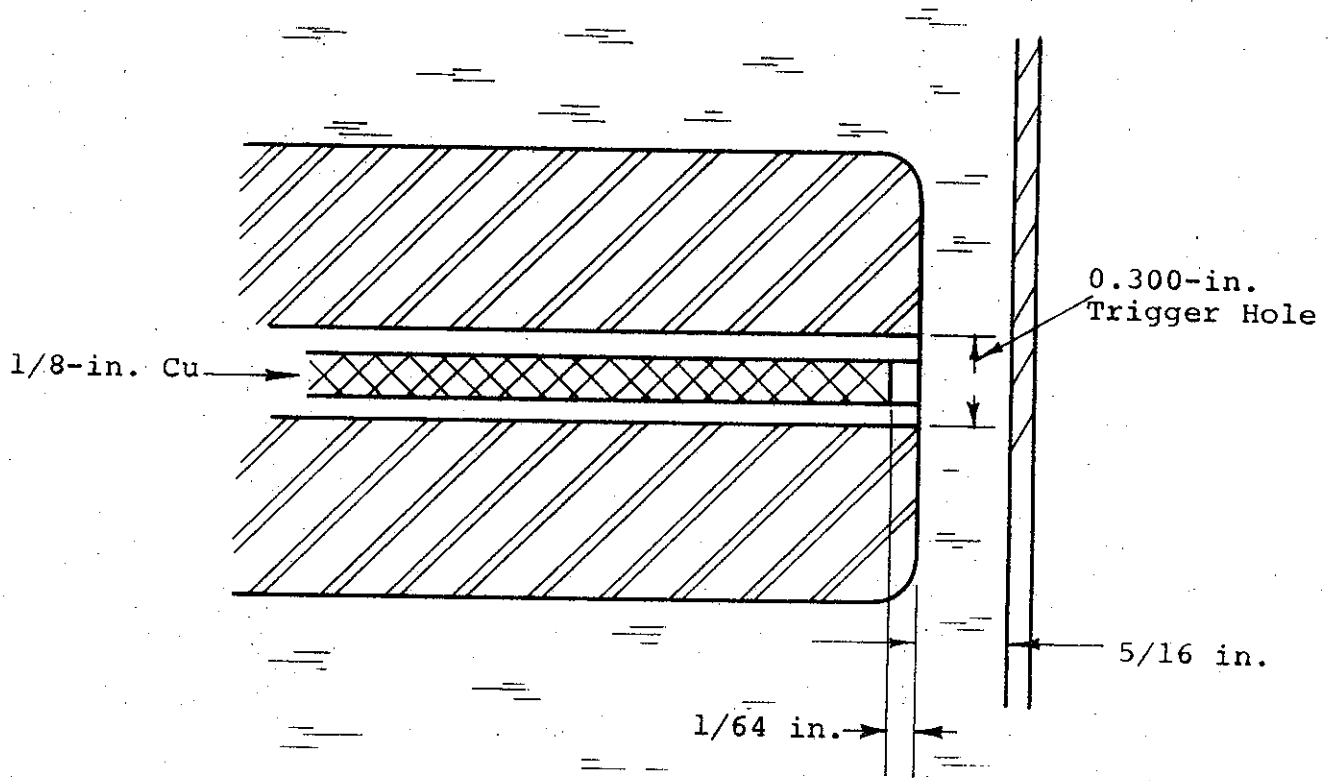


FIGURE 1. WATER TRIGATRON

The trigger pulse then forms a plasma which expands into the region between the main electrodes until the electric field at the surface of the plasma exceeds the breakdown strength of the gas. An additional feature is that the breakdown between the main electrodes is made prompt and regular by ions and electrons from the plasma, which subjects the entire gap to ultraviolet radiation.

By contrast, in liquids the breakdown proceeds relatively slowly by means of streamer propagation. Electric field strengths of the order of 500 kV/cm may be achieved for times of the order of 1 μ sec, but the breakdown process actually begins at electric fields as low as about 100 kV/cm. The higher electric field will certainly need to be present if the trigatron is to close in the time short enough that the jitter is of the order of nanoseconds and the switch is therefore only of interest in the pulse-charged application.

The most probable mechanism for initiating a rapid breakdown in the main switch from the trigger spark is that streamers are formed in the high-field region by the trigger breakdown, and these streamers are rapidly accelerated toward the opposite main electrode. A much higher-voltage trigger pulse is necessary in liquids than in gases in order to break down the trigger spark gap and also to supply the extra energy necessary to heat the denser material.

Assuming the trigger pulse would be sufficient to start the breakdown across the main electrodes of the trigatron, the polarities of these electrodes were chosen to minimize the transit time, and hence the jitter of the arc. This assumption probably applies those polarities which would allow the greatest electric field

across the electrodes. Water exhibits a strong polarity effect that allows the field on the negative-enhanced electrode to be about double that possible on the positive-enhanced electrode before the enhanced electrode becomes the source of the breakdown. Since the trigger pin and trigger hole will produce some field enhancement in an electrode that contains them, it appears that this should be the negative electrode. There remained the choice of trigger pulse polarity. Because of the polarity effect and the field concentration on the trigger pin, the latter would spark to its surrounding electrode much more easily if a positive pulse were applied, as was actually used. If the trigger pin were pulsed negative, it would experience a high field toward the opposite (positive) main electrode, which may have an advantage; however, it is then most likely that the main spark current will be directly to the pin, and that the pin and insulator will be damaged.

Most tests were conducted with the trigger electrode in the negative main electrode and a positive trigger pulse; however, in addition, the main polarity was inverted, which degraded the self-breakdown of the switch, as expected. Only a positive trigger pulse was attempted, since a negative pulse would in this case be a disadvantage in all respects.

A. APPARATUS

1. 2/3-Ohm Coax

Originally the objective of the work was to install six trigatron switches into a coaxial water line with a 2/3-ohm characteristic impedance, a pulser built and owned by Physics International (see Figure 2), and used to test the concept of multiple-

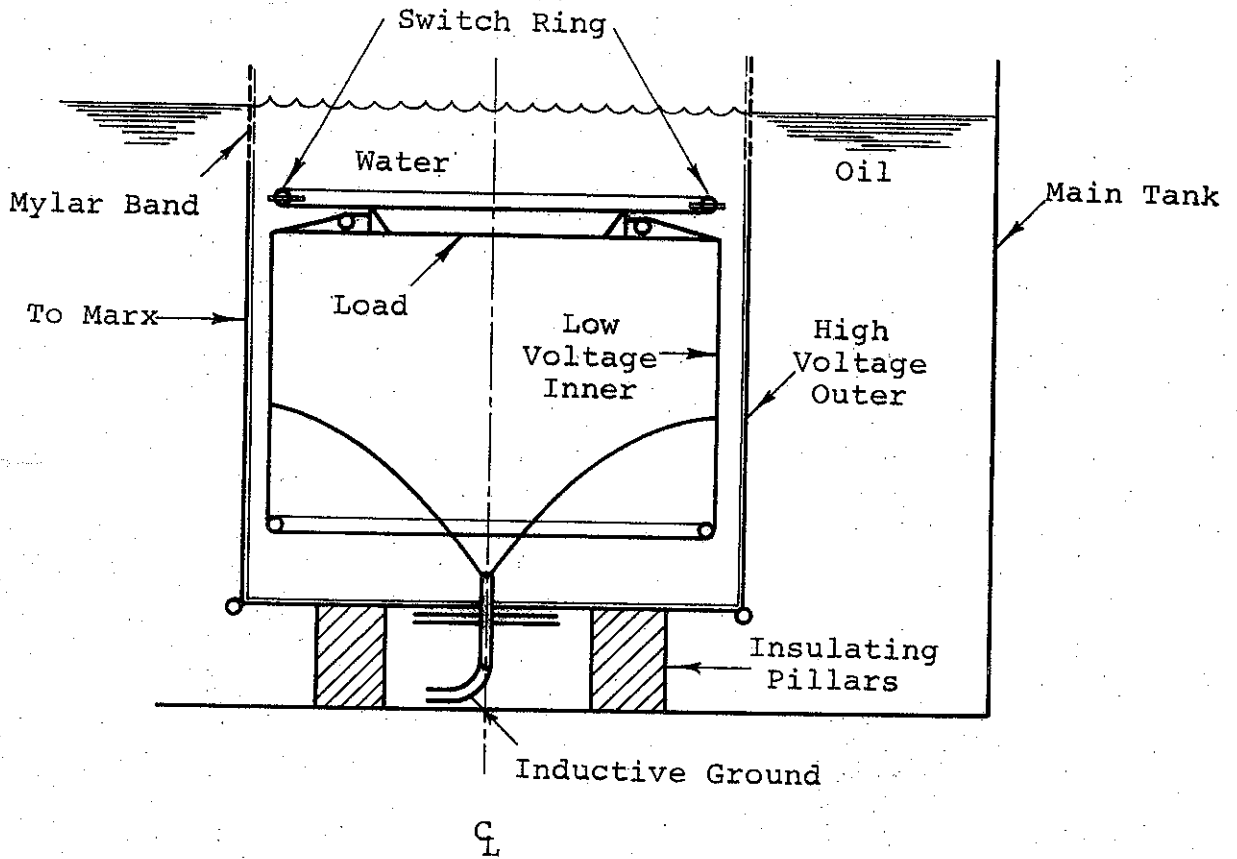


FIGURE 2. PHYSICS INTERNATIONAL'S WATER PULSER

channel, self-closing water switches, and to perform preliminary research on very high current (greater than 500 kA), low-impedance diodes. Pulse duration was 100 nsec and the line was charged to a maximum voltage of 900 kV. Typical output pulse into a matched load is shown in Figure 3. Tests have shown that the high rate of charging necessary to obtain sufficient spark channels in the self-closing multichannel switch also produced in this geometry a pre-pulse that limited the operation of the tube. It was hoped that successful development of the trigatron switches would circumvent this difficulty.

Toward this end, the coaxial water pulser was modified to accept six trigatron switches by rebuilding the switch ring (Figure 2).

2. Prototype Test Apparatus

At the same time, a small experimental area was prepared in which individual prototype trigatrons would be tested until there was sufficient confidence in the design to warrant installation in the large pulser. These experiments took place in a small steel tank filled with de-ionized and degassed water (Figure 4). The capacitance driving the trigatron switches was formed by a 10-sq-ft aluminum saucer resting on three sheets of 1/4-in. polyethylene on the floor of the tank. Much of the capacity between the saucer and the tank was due to energy stored in the water rather than the polyethylene; thus an exact calculation of the total capacity was impossible. However, by measuring the period of charge of the capacitor from a Marx generator of known inductance, an empirical measurement of 18 nF was made.

The Marx generator used was a specially constructed 6-stage device vertically stacked in air. Each stage of the Marx had a capacitance of 1 μ F and the inductance of the energy-storage

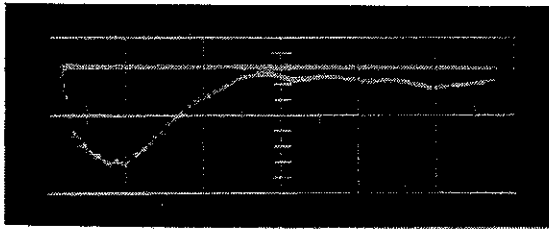


FIGURE 3. WATER PULSER OUTPUT INTO MATCHED LOAD (100 nsec/cm, 200 kv/cm)

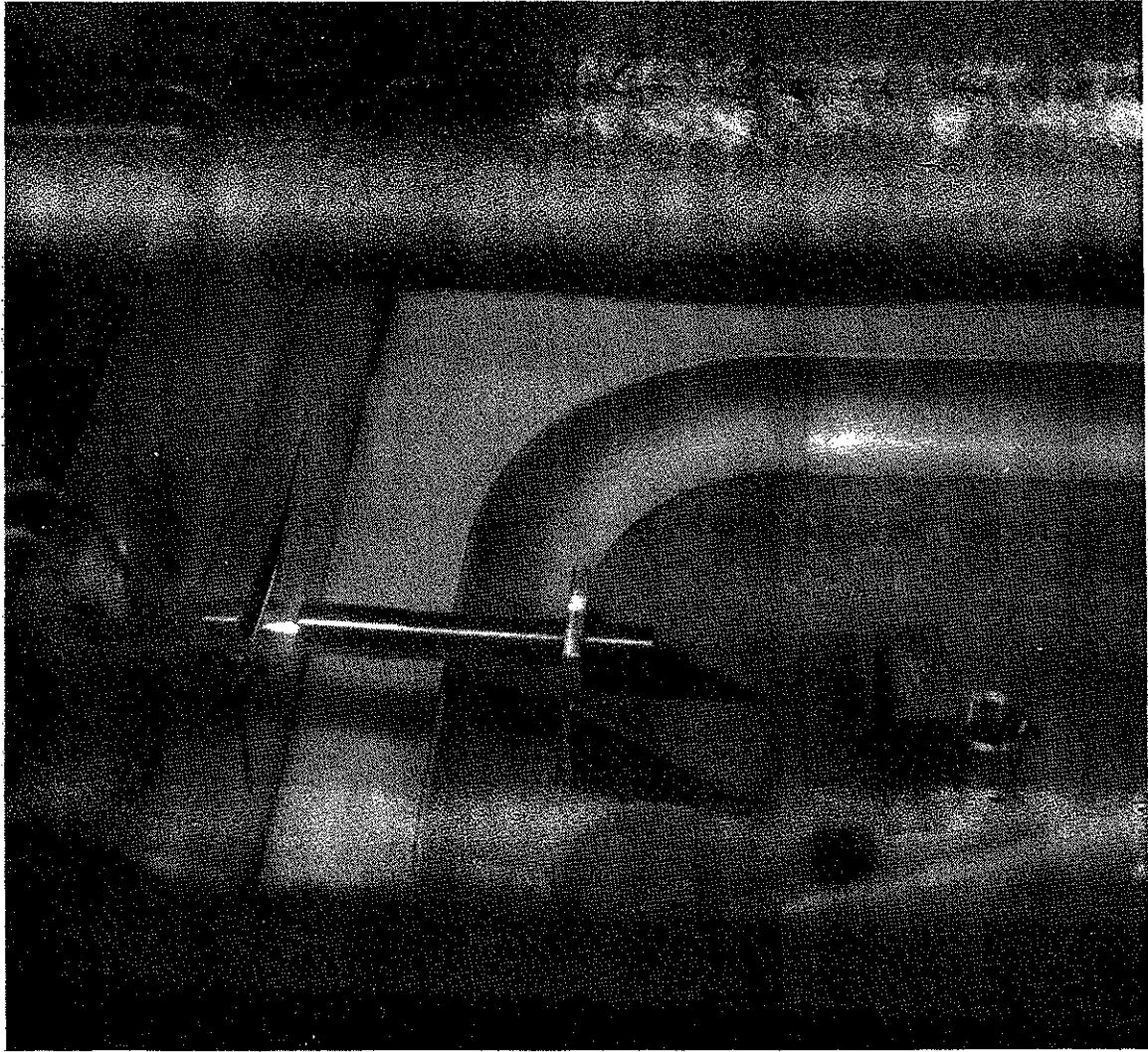


FIGURE 4. TRIGATRON FIRING IN WATER

section was small compared with very large inductance of 150 μH between the Marx and the aluminum saucer. The chief purpose of this inductance was to slow the risetime of the voltage on the trigatron to a value typical of high-energy low-impedance pulse generators such as the 2/3-ohm line. The configuration served a second purpose in that the erection of the Marx produced a fast rising voltage on the input side of the 150- μH inductance. A carbon resistor/divider was used to inject about 20% of this transient voltage into a cable delay line. The pulse was extracted after a suitable length of time to trigger the generator that supplied the trigger pulse to the trigatron.

To simulate the surface to which the trigatron would switch, a clean stainless-steel sheet was fixed to the wall of the water tank. When the surface became greatly pitted, the sheet could easily be replaced. The trigatron itself was attached to the aluminum saucer. Later in the experiment the trigatron electrode was fixed to the ground-potential tank and switched to the high-voltage potential of the capacitor.

3. The Trigger Pulser

The operation of the trigatron depends on generating a trigger arc of sufficient intensity and duration to cause the breakdown of the switching medium between the high-voltage electrodes. A schematic of the pulser constructed to provide the trigger spark is given in Figure 5 and a diagram of it in Figure 6. Since it was planned to run six switches simultaneously, the trigger pulser had six output cables each 60 ft long.

Two 1- μF , 25-nH, 50-kV capacitors charged plus and minus in series were switched into the six parallel cables by a single midplane-triggered gas switch. The capacitors, the gas switch,

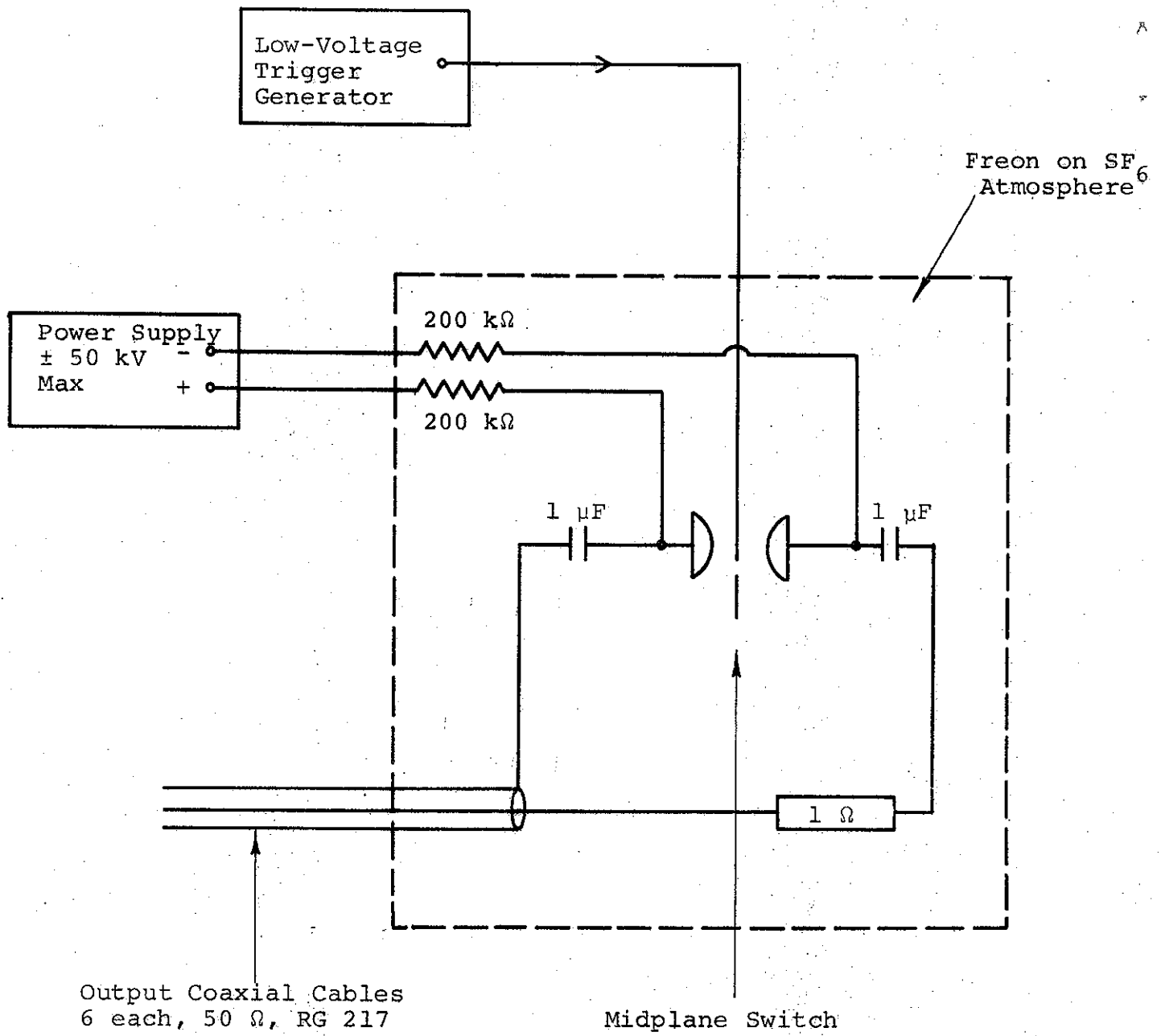


FIGURE 5. TRIGGER PULSER

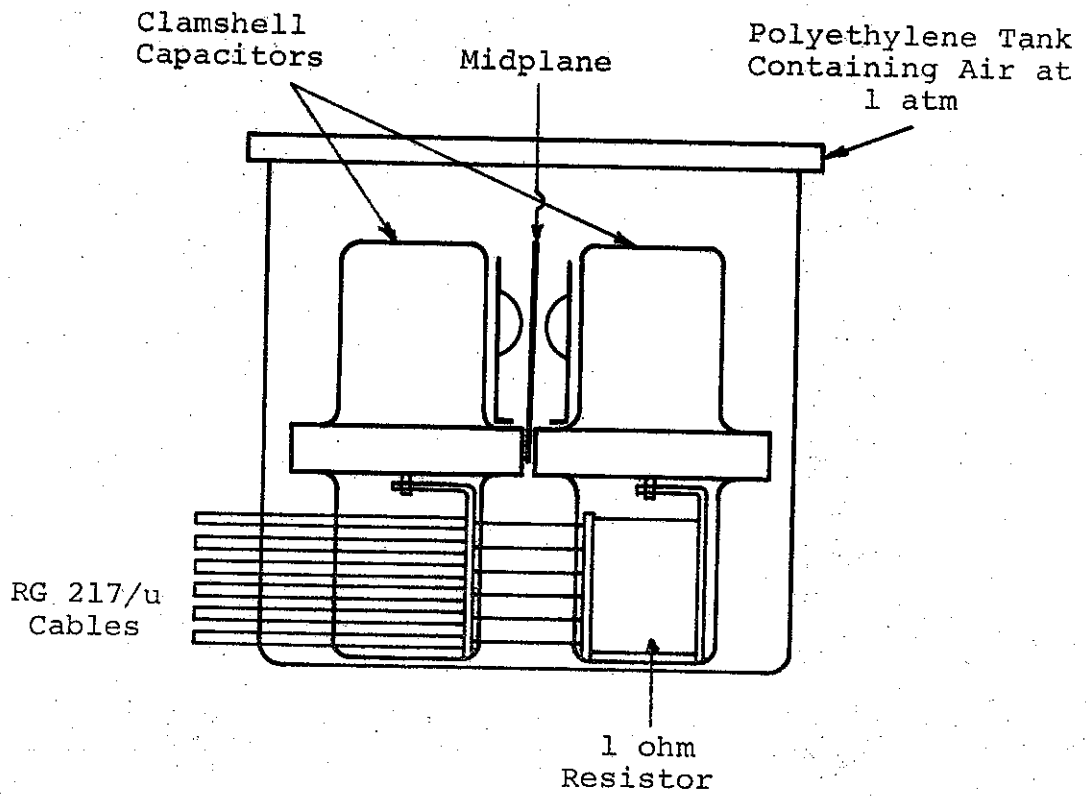


FIGURE 6. TRIGGER PULSER ASSEMBLY

and the input ends of the cables were contained in a polyethylene box that could be filled with SF₆ to obtain full charging voltage of plus and minus 45 kV (Figure 7). Freon was initially used for this purpose but after a number of discharges, sufficient carbon was formed by decomposition of the Freon to track the inside surface of the polyethylene container.

The gas switch was triggered by applying to the mid-plane electrode the part of the output pulse from the Marx erection that had been fed through the cable delay line. Thus, the trigger generator was always triggered at a fixed time after the start of the pulse charge of the trigatron.

The risetime of the trigger pulse supplied by the cable pulse generator was 10 nsec. At the output end of the cables, voltage doubled when the pulse reached an open circuit. Measurements confirmed that an amplitude as much as 175 kV was produced.

In tests on the single switch in the prototype experiments, all the cables were connected in parallel at the output for convenience, and an 8-ohm series resistor was added to the parallel combination, giving approximately 16-ohms impedance at the trigatron switch. It was reasoned that if the driving impedance were low, more voltage drop would be maintained across the trigger arc and further extension of streamers from the trigger arc toward the main gap might take place. Should this have proved desirable, a similar impedance could be used to drive each of the six individual trigatrons by adding more cables in parallel to the trigger pulser.

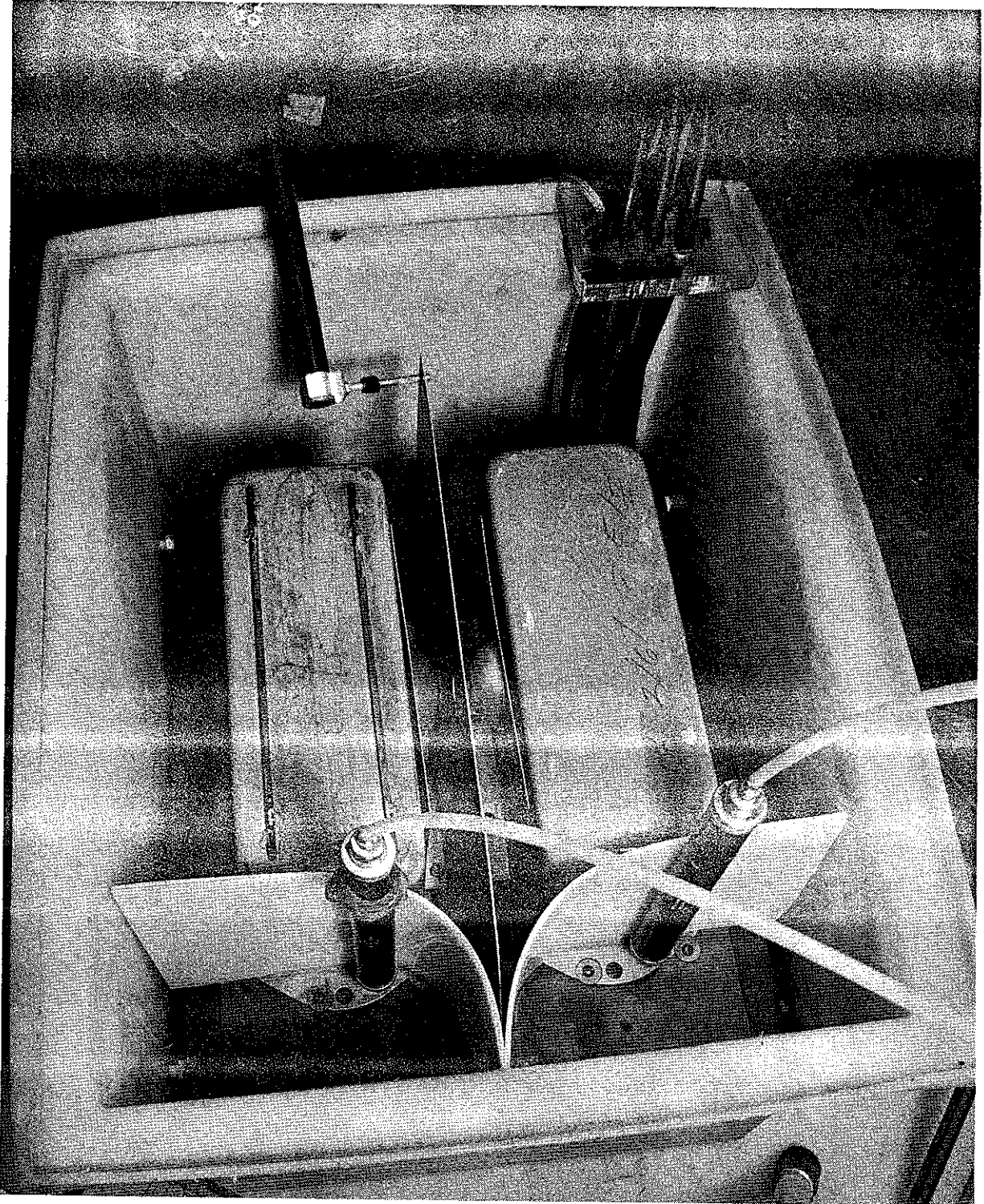


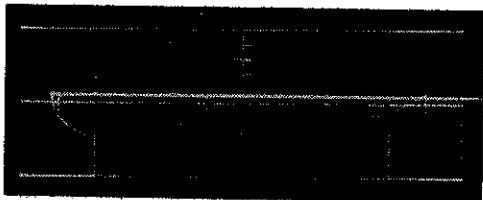
FIGURE 7. TRIGGER PULSER AND COILED LINE

R8694

4. Monitors

Three current probes were built for two different purposes-- two B-loops for monitoring the breakdown in the main gap of the trigatron and a Rogowski loop for monitoring the trigger pulse. One of the B-loops had a split shield and the other was unshielded. The signals from the B-loops were integrated at the loop by low-inductance resistors and they appeared to differ only in amplitude (Figure 8).

B-field monitors were sufficient for measuring the time between the current pulse across the trigger and current pulse across the trigatron (i.e., the delay between trigger and closure of the switch). However, they were able to measure neither the trigger voltage nor the voltage applied across the trigatron. To measure pulsed voltages, copper sulfate monitors were used. Their frequency response was limited to less than 100 MHz. The copper sulfate monitors were calibrated several times during the experiment to ensure their accuracy and the voltage response was constant.



~60 kA/cm on Vertical

50 nsec/cm on Horizontal

FIGURE 8. WAVEFORM FROM THE INTEGRATED,
UNSHIELDED B-LOOP

B. EXPERIMENTAL RESULTS

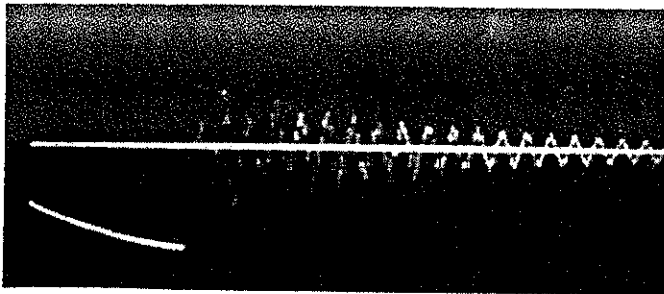
1. Self-Breakdown Tests

The first test with the prototype trigatrons was to determine self-breakdown behavior, namely breakdown without applying a trigger pulse. The tests had two purposes: first to determine the effect of the geometry of trigger insulator and trigger pin on the breakdown strength of the main gap; and second to find what distance the switch electrodes should be placed away from each other at a given voltage to ensure the greatest electric-field strength without danger of firing before application of the trigger.

With a steel rod filling the trigger hole, the overall gap strength was observed to be 280 to 320 kV/cm, with negative polarity on the field-enhanced electrode (Figure 9). When the hole was filled with water, or with nylon flush with the face of the trigatron, or with ceramic flush with the face, the gap behaved identically. But when the insulator extended only 1/16 in. beyond the face, the gap strength was degraded and the insulator was chipped by the spark. This effect was not unexpected. Because of the high dielectric constant of water, any dielectric that intersects the field lines between the electrodes of the trigatron is highly stressed, and so is the nearby water.

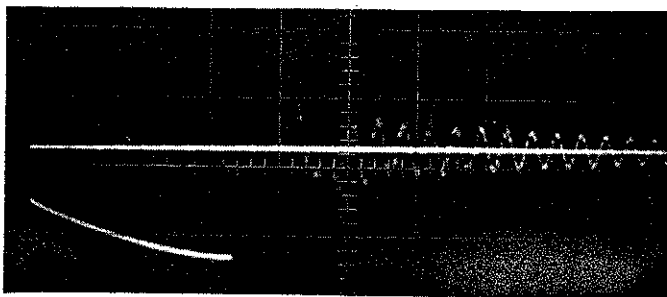
2. Insulator Tests

The first tests of the trigger insulators showed that it was necessary to add a series resistance of 8-ohm to limit the current from the trigger circuit ringing so as not to destroy the insulator every shot. This damage occurred with whatever insulator was used. The 8-ohm had little effect on the trigger-pulse and risetime and dropped the current by only $\approx 50\%$.



a. Trigger Hole Filled by Steel Rod
1/4-in. Electrode Spacing

140 kV/cm 500 nsec/cm



b. Trigger Hole Filled by Nylon Rod
1/4-in. Electrode Spacing

140 kV/cm 500 nsec/cm

FIGURE 9. SELF BREAKDOWN TESTS

Four types of insulation were used around the trigger pin: ceramic, nylon, polycarbonate, and polyethylene. A typical configuration is shown in Figure 10. Ceramic insulators were used by Nesterikin; however, when used in our experiments, they broke very easily and could not be used for many shots. Ceramic seems an unlikely material for this application because of its brittleness. The reason ceramic was used by the Russians is that they possibly used it in previous gas trigatrons, in which the shock waves generated are weaker. The advantage of the ceramic in the gas trigatron is that it has a high dielectric constant, which generates a very high field around the point of the trigger pin and allows the gas to be broken down very reproducibly. The high-energy density stored in the ceramic at the time of breakdown and its resistance to erosion may also be significant. In a water application the high dielectric constant helps to keep down the electric field in the solid, but this advantage is outweighed by its brittleness.

3. Trigger-Gap Jitter Studies

Figure 11 is a complete set of oscilloscope traces showing all the important events in the firing of the trigatron. The delay $t' - t_0$ until the onset of trigger-gap current had a jitter of 10 to 15 nsec.

It was thought possible that this jitter would contribute to the overall switch jitter depending on whether the main switch closure relates to the appearance of voltage across the trigger gap or its closure. There were three possible ways of improving the trigger breakdown jitter: (1) increase the voltage, (2) make the trigger gap smaller, or (3) sharpen the trigger pin. None of these

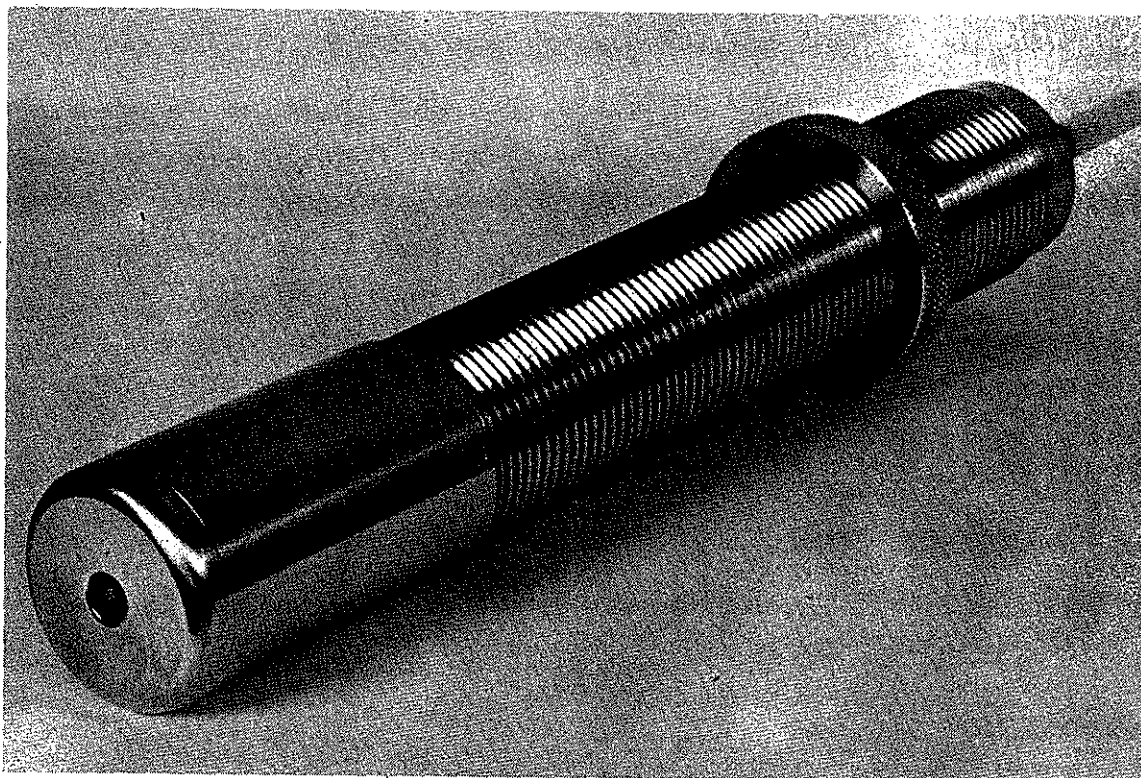


FIGURE 10. TRIGATRON ELECTRODE WITH TRIGGER

would have produced untainted benefits, however. Increasing the voltage might have led to frequent insulator failure and, moreover, should not have been necessary since we already had 175 kV rising 10 nsec, compared with the 100 kV rising in 30 nsec reportedly used by Nesterikin in the U.S.S.R. Making the trigger gap smaller would have led to less disturbance in the field in the main gap, and thus caused more jitter in the closure of the trigatron. Sharpening the trigger pin would have shortened its life and probably not changed the jitter noticeably. Therefore, even though the trigger jitter was somewhat large, it was concluded that the design was adequate for the prototype phase of testing.

4. Triggering Studies

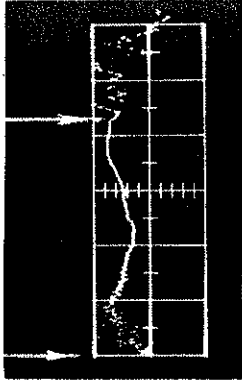
In a typical experiment in which the triggering of the main gap was studied, the sequence of events is as follows: (1) the trigatron gap is pulse charged; (2) the trigger generator is fired with the correct delay to deliver a trigger pulse at the trigatron tip when the full pulse charge appears across the gap (the onset of the trigger voltage and the breakdown of the trigger gap is monitored); (3) the breakdown of the gap is monitored by voltage and current monitors. When 2 and 3 occur in reverse order, the trigger pulse arrives too late to produce an effect; this is called a self-fire--early. In fact, when the breakdown occurs within 40 nsec of the arrival of the trigger the event probably is a self-fire--early, because the delay in firing the trigger pin is 40 nsec plus or minus 10 nsec jitter.

It is important to note that the voltage across the trigatron was very nearly the same, shot-to-shot, at the instant the trigger pulse arrived. This was a result of low jitter in the midplane switch of the trigger pulser and eliminated one possible source of error in the experiment.

In Figure 11 (a, b, c, and d) various oscilloscope traces from the trigatron experiment can be seen. Generally we monitored either the trigger voltage (Figure 11a) or the trigger current (Figure 11b). To indicate where the trigger gap closes we have placed t' . This occurs 40 nsec after the arrival of the trigger pulse leaving the current on for about 120 nsec. Alternatively, the trigger current or the voltage waveform triggers another scope that subsequently displays the current produced across the main gap (Figure 11c). A further confirmation of the trigger delay is evident from the main-switch voltage waveform, on which the onset of the trigger current produces a slight ripple (Figure 11d). The closure of the main water gap which discharges the 18-nF capacitor is marked at time t' . As all the waveforms indicate, the delay in trigatron closure ($t_0 - t''$) may be as much as several hundred nanoseconds. Indeed, on many shots no degradation of the usual self-breakdown can be ascribed to the trigger spark.

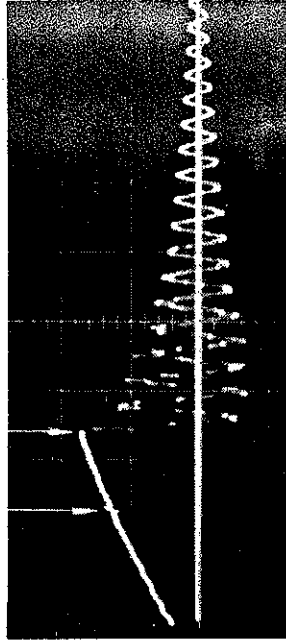
Tests were performed chiefly with the preferred polarities with the trigatron electrode negative and the trigger pin subjected to a positive trigger pulse. A gap spacing of $\frac{1}{4}$ in. and a voltage of 200 to 250 kV was usually chosen. Many configurations differing in insulator material and position of the tip of the trigger pin were tested. In the majority of tests, detailed statistics were not accumulated; rather, some indication of a definite triggering action was sought, but if shown to be absent by shot-to-shot variations of the order of 100 nsec then an experimental parameter was changed to effect an improvement. Many tests were made difficult or impossible by insulator failure and successive configurations were eliminated as possible designs for a useful switch. Eventually reversed trigger polarities were tested (negative trigger pulse), then reversed polarities on the main dielectrics (positive trigatron). The last polarity reversal

t' t''



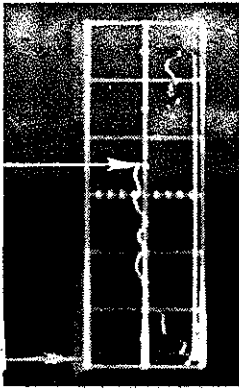
b. Onset of Trigger Current (100 nsec/cm)

t' t''



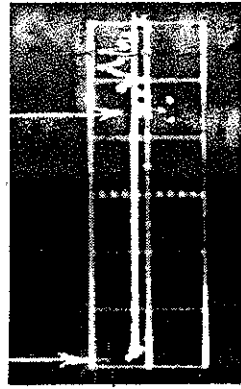
d. Pulse Charge (500 nsec/cm)

t₀ t'



a. Trigger Pin Voltage (120 kV/cm, 20 nsec/cm)

t' t''



c. Main Gap Current (100 nsec/cm)

FIGURE 11. TRACES SHOWING EFFECT OF THE TRIGGER PULSE ON TRIGATRON

required the switch spacing to be increased to withstand the same voltage. Having shown that any configuration would unlikely provide a switch with a jitter of the order of a few nanoseconds, it was decided to conduct a final test to decide if any triggering action could be detected at all. This test was performed with the trigatron electrode negative and the trigger pulse positive; the trigger pulse was applied at a point so close to the average self-fire that on numerous occasions the self-fire was actually entirely before the trigger-spark closure.

The data compiled in this experiment under the conditions illustrated in Figures 12 and 13 is presented in Table I and illustrated in Figure 14. By merely looking at the shots in which a 150-kV trigger pulse was used, there is no indication as to whether or not the trigatron broke by itself or the trigger pulse was effective. Therefore, a control experiment was performed in which the trigger pulse was shorted.

As can be seen in Figure 14 the difference produced by the trigger pulse is not great. Disregarding those shots that could not have been triggered (delay less than or equal to 50 nsec, since 40 nsec is the portion of the delay attributable to breakdown of the trigger gap), the average delay of the main-switch breakdown from the arrival of the trigger pulse is reduced from 200 nsec to 125 nsec by the trigger pulse. The error on the mean values are about 35 and 20 nsec, respectively, and the reduction is probably significant. Thus the trigger pulse probably produces an effect but the jitter is so large that for practical purposes the switch is not useful. The jitter is 70 nsec when the trigger pulse is applied and 90 nsec in the control test.

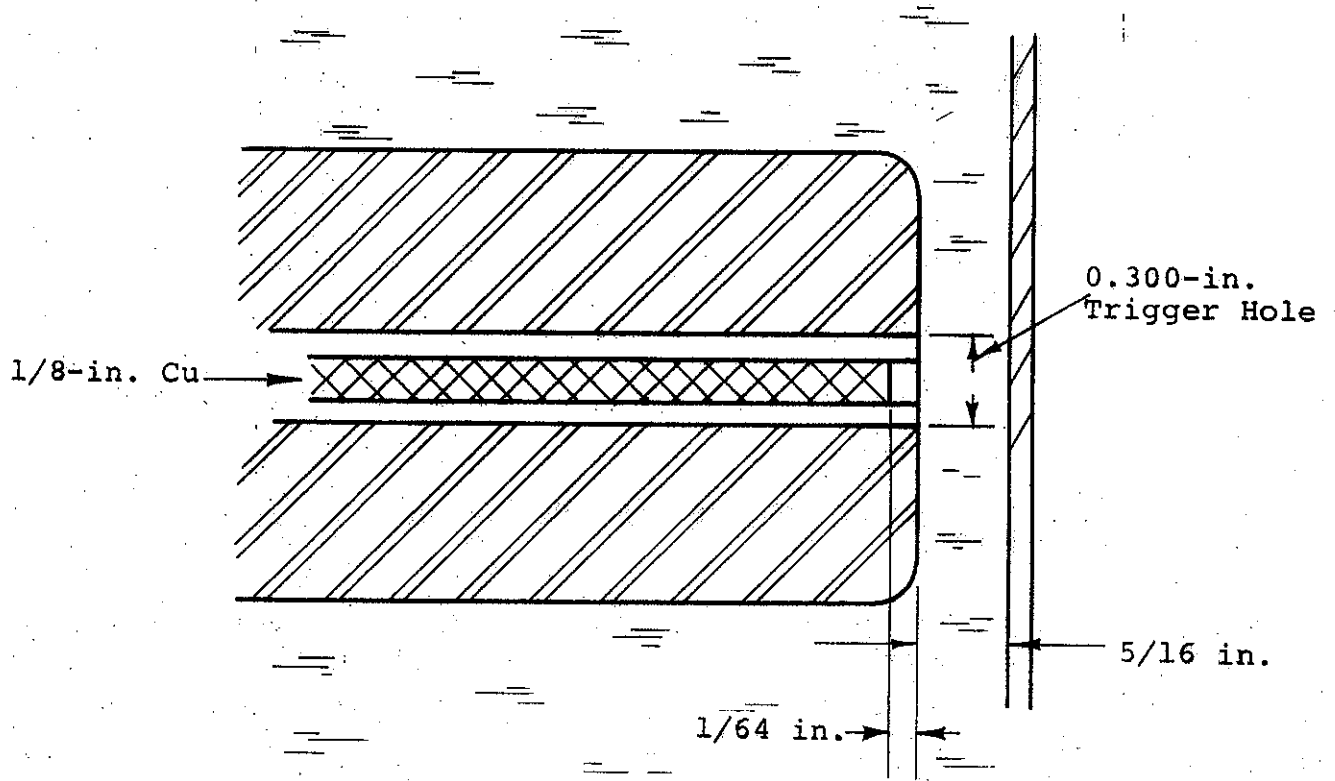


FIGURE 12. TYPICAL EXPERIMENTAL CONDITIONS

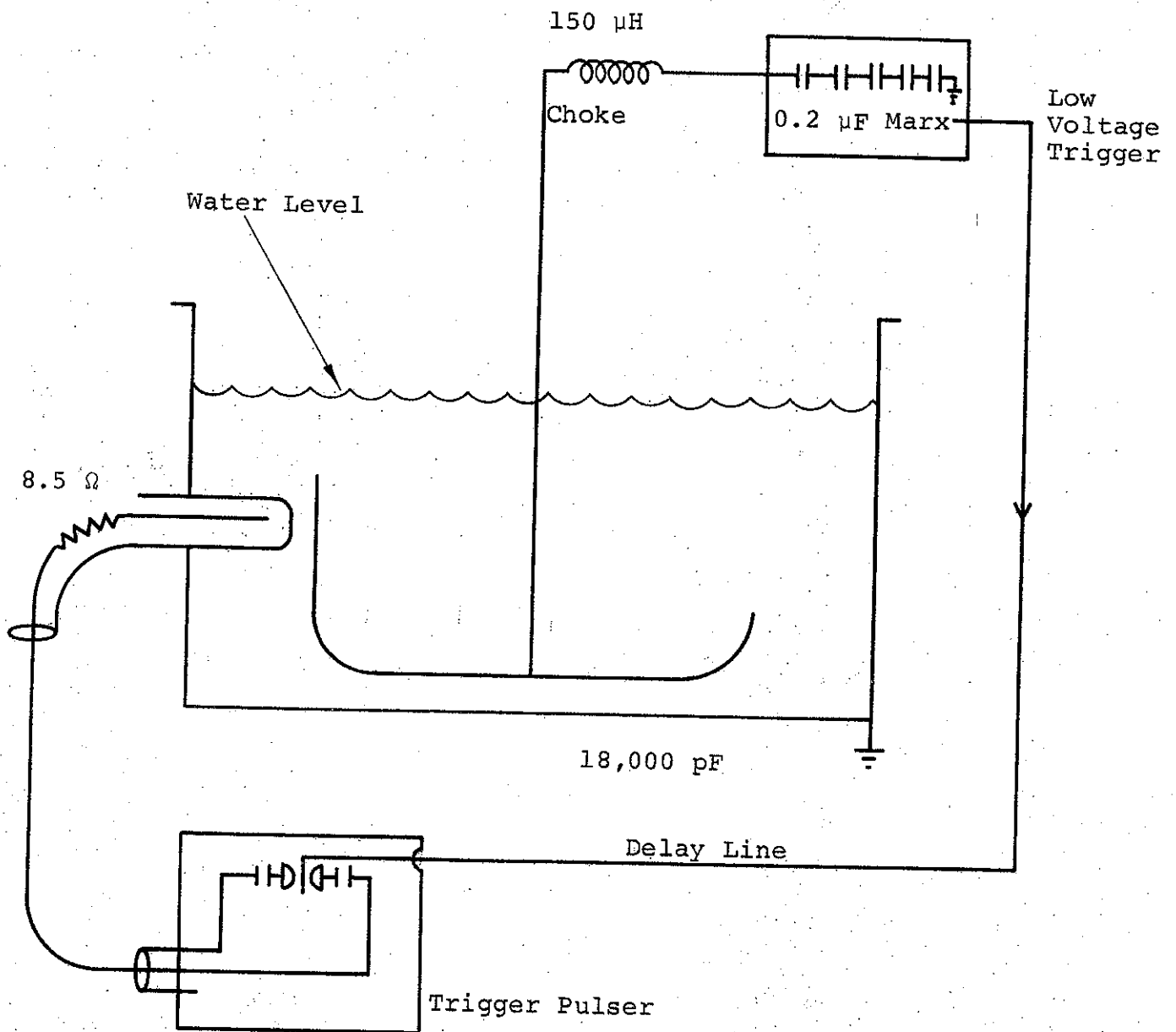


FIGURE 13. SETUP FOR TRIGATRON EXPERIMENTS

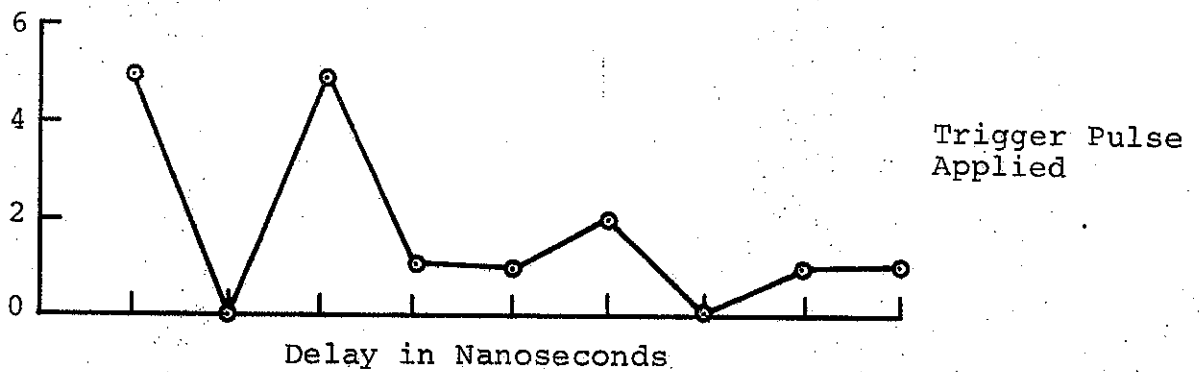
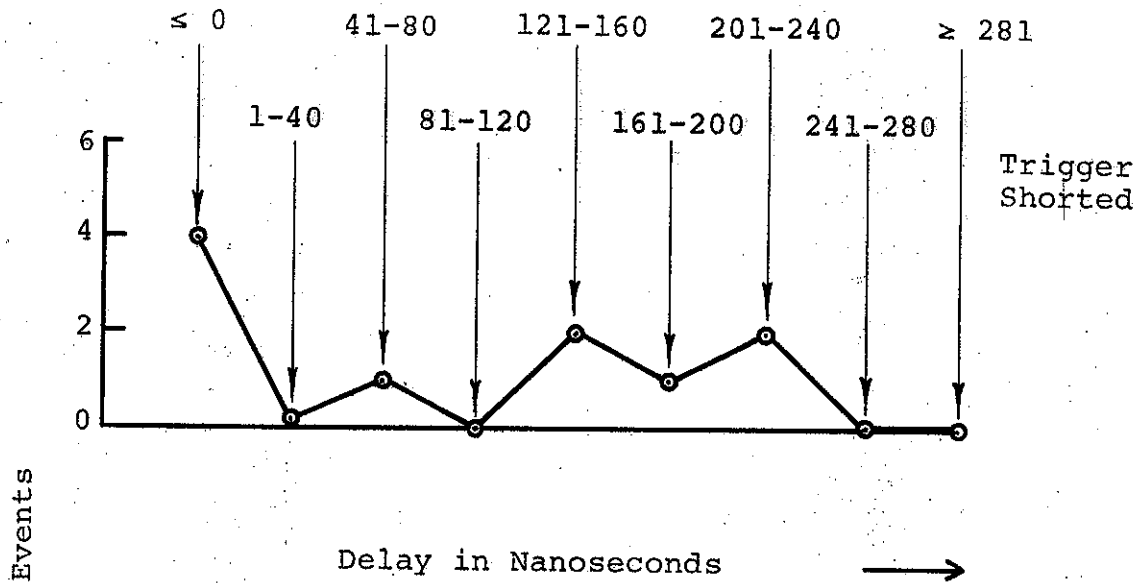


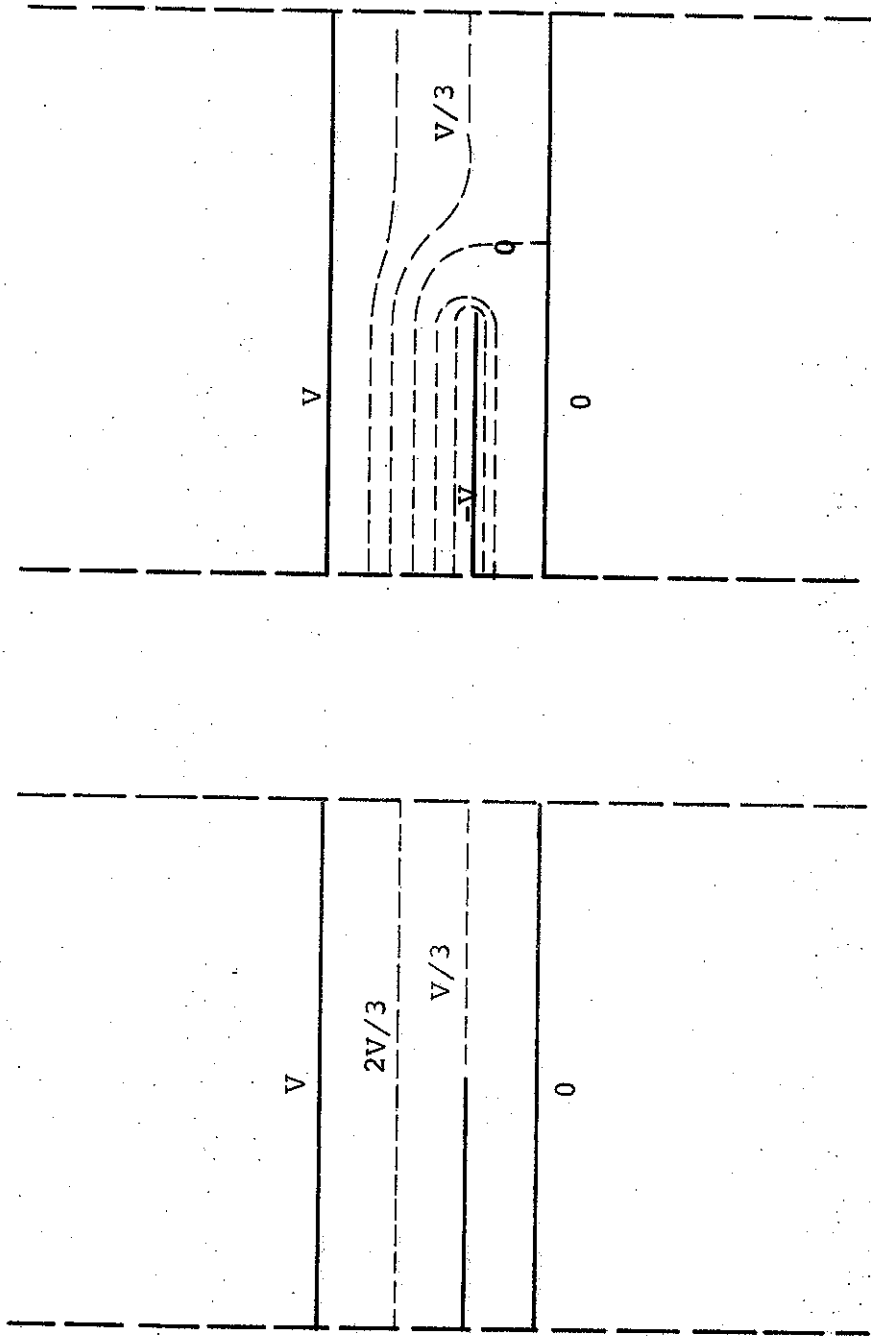
FIGURE 14. FREQUENCY OF TRIGGERED AND NON-TRIGGERED DELAYS

TABLE I

Shot No.	<u>Trigger Pin Shorted</u>		<u>Trigger Pin Not Shorted</u>	
	Delay ($t'' - t_o$) * (nsec)	+15kV Breakdown Voltage (kV)	Delay ($t'' - t_o$) (nsec)	+15kV Breakdown Voltage (kv)
1	150	215	90 ⁽²⁾	255
2	230	241	-160	200
3	-400	168	-70	214
4	350	238	75	238
5	0	214	60	233
6	-450	150	65	215
7	-70	207	265	238
8	200	230	175	232
9	150	223	165	229
10	385 ⁽¹⁾	224	<300	245
11	75	221	95	224
12	-100	200	-170	196
13	210	224	10 ⁽²⁾	232
14			45	233
15			-120	210
16			-20	215
17			70	228
18			160	238

* t_o is taken to be the moment of the onset of voltage at the trigger pin, t' to be the onset of current at the trigger gap, and t'' the onset of current of the main gap.

- (1) Trigger pulse applied early, when voltage on gap was <210kV
(2) Trigger pulse applied late, when voltage on gap was >230kV



(a) No Trigger Disturbance (b) With Trigger Disturbance

FIGURE 15. THREE ELECTRODE FIELD ENHANCED SWITCH

this case, $V/3$ is the "balanced" potential for the middle electrode. If the middle electrode is made to assume a different potential by a trigger pulse, such as $-V$ (Figure 15b), then the field lines would be no longer uniform, but would be highly concentrated around the edge of the middle electrode. In the highly stressed condition, the middle electrode to outer electrodes becomes a point plane gap, for which the transit time of the arc may then be estimated from the formula taken from J. C. Martin:

$$Ft^{1/n} d^{1/6} = Kp^m$$

where

d , in cm, is the distance, V_0 is the voltage in MV
 $F = V_0/d$ is the working field in MV/cm, and
 t is the closure time in μsec .

The exponent, n , decreases from about 6 in atmospheric SF_6 to about 2 at very high pressures, while m increases from about 1 to about 6 and K depends on polarity.

Clearly, t is a strong function of the gas pressure, working field, and polarity, but is typically less than 10 nsec, while the jitter may be expected typically to be 1 nsec or less.

Trigger-electrode-potential $V/3$ was chosen because it maximizes the field which can be obtained on triggering. For a $V/3$ three-electrode switch with a trigger potential of exactly $-V$, it is unpredictable in which gap of the switch the arc will form first, because the fields in both sides are $3V/d$, or an increase over 3:1 over the untriggered value. A smaller trigger voltage, $<-V$, would break the larger gap first and a larger trigger voltage would break the smaller gap first. If the large

gap breaks first (desired case), the middle electrode assumes a new potential, usually very close to V , depending on impedance driving the switch and the trigger impedance. The smaller gap then has a field of $3V/d$ again and breaks soon after. Making the gaps more equal would decrease the working field when the second gap fires, while making them more unequal would decrease the working field that can be applied to trigger the first gap in the normal order (larger gap first, smaller second). In practice, polarity effects will also affect which side breaks first and optimum designs may depend on the polarity of the applied voltage.

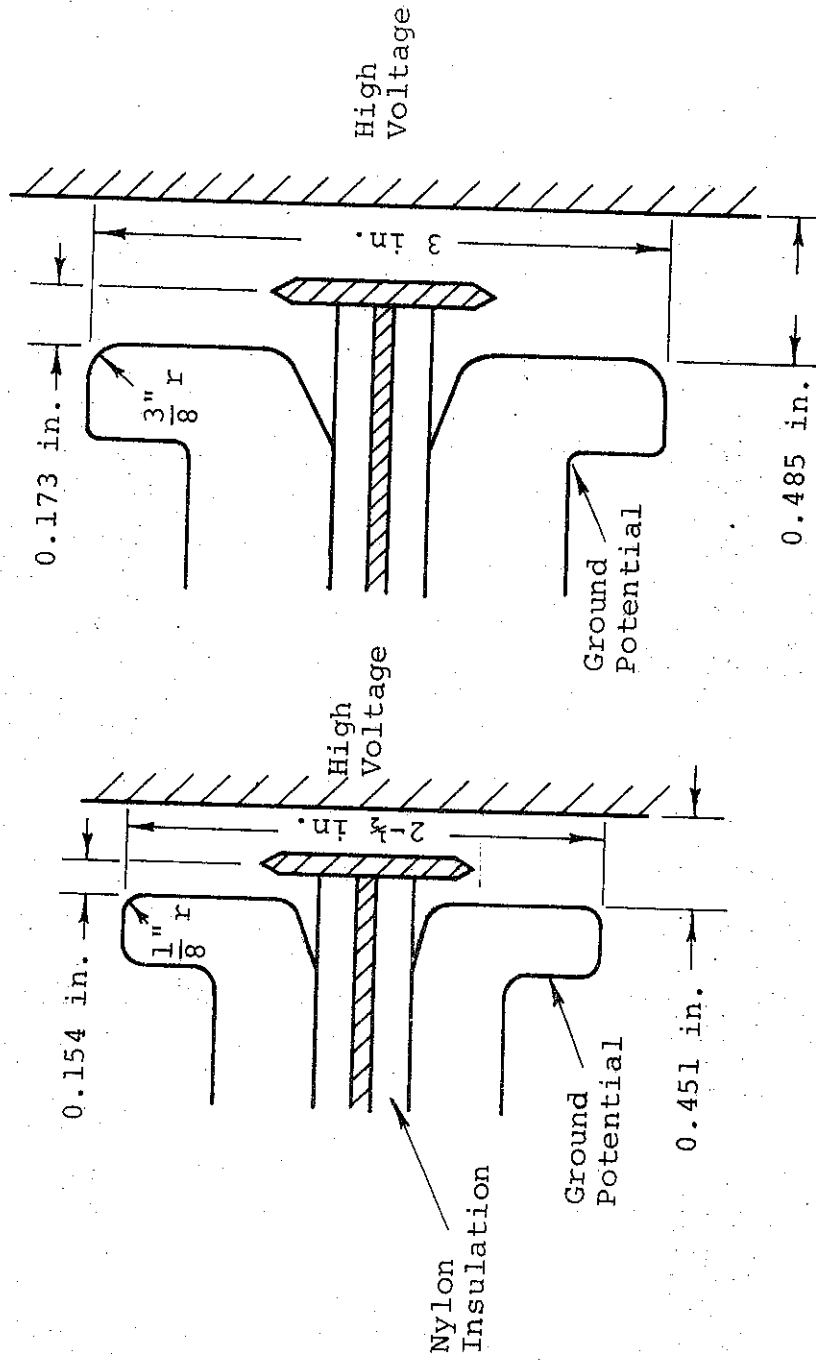
A. APPARATUS

1. Three-Electrode Switches

Two switches were constructed for preliminary testing in the range of 300 kV. For optimum performance, the $V/3$ position was chosen for the middle electrode.

In Figure 16 a section cut through the axis of symmetry represents the two switches tested. The middle electrode had a coaxial feed and a knife edge. Silver soldering was used to get a good connection between the thin, $1/16$ in., middle electrode and the rod down the center. All corners were radiused, especially around the gas/solid interfaces. To reduce the probability that the center insulator would track, the conductor was countersunk, decreasing electric fields on the interface. Shown in Figure 17 is the gas envelope, a plexiglass cylinder 6 in. long, with a 5 in. o.d.

Many parts intended for the trigatron experiment were used to build the three-electrode switch. The SF_6 switches were also designed to be possibly used in the $2/3$ -ohm water line, if success warranted and time permitted.



a. b.

FIGURE 16. PROTOTYPE THREE-ELECTRODE SF₆ SWITCHES

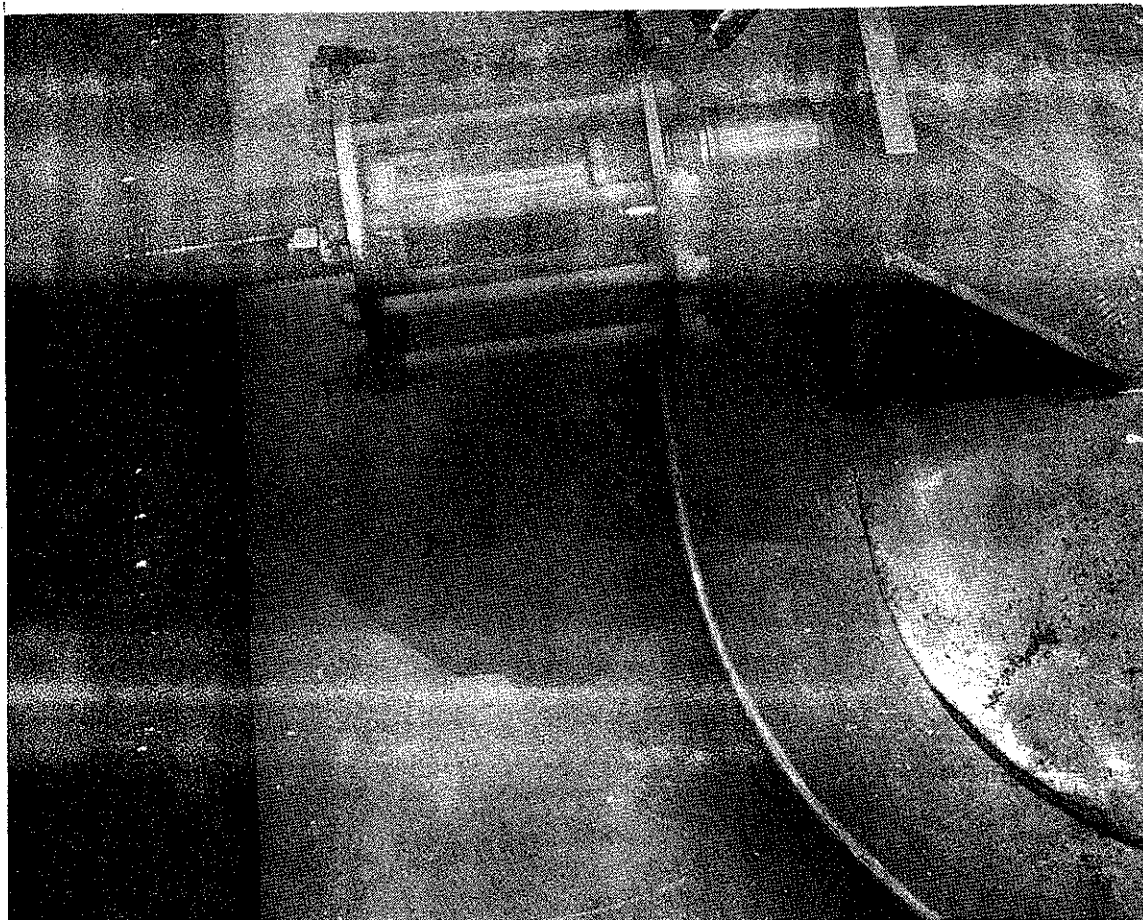


FIGURE 17. PROTOTYPE SF₆ SWITCH FIRING IN WATER

2. Trigger Pulser and Isolation Gap

The same trigger pulser from the trigatron work was used. However, the pulser could not be directly connected to the middle electrode, since it would pull the latter to ground potential. A small uniform-field gas gap was built that could be adjusted by either changing the spacing or gas pressure to withstand the potential difference between the middle electrode and the trigger pulser; this gap breaks promptly when the potential is changed by the arrival of a trigger pulse and is called the "isolating gap."

Initial tests were with a dc charge across the switch and a Blumlein trigger pulser (Figure 18). This consisted of two 60-ft lengths of RG217 cable, the outer shields of which were charged to the full potential of the switch. In these first tests the trigger was fired by closing the switch between the outer shield and a grounded inner conductor.

B. RESULTS

1. Self Fire Tests

A resistive divider was used to keep the middle electrode at $\approx V/3$ before triggering. The total values of the resistors required was determined by the rate at which the switch was charged as compared to the rate at which the resistors could discharge the capacitive imbalance of the trigger electrode. Although the resistive division ratio should be approximately the ratio of the distances between the middle electrode and the outer electrodes, the best ratio was determined by experiment. The ratio that maximized self-breakdown strength was used.

At first, tests were taken with dc voltages up to ± 120 kV and later pulse charged using the Marx. Both prototypes (Figure 16)

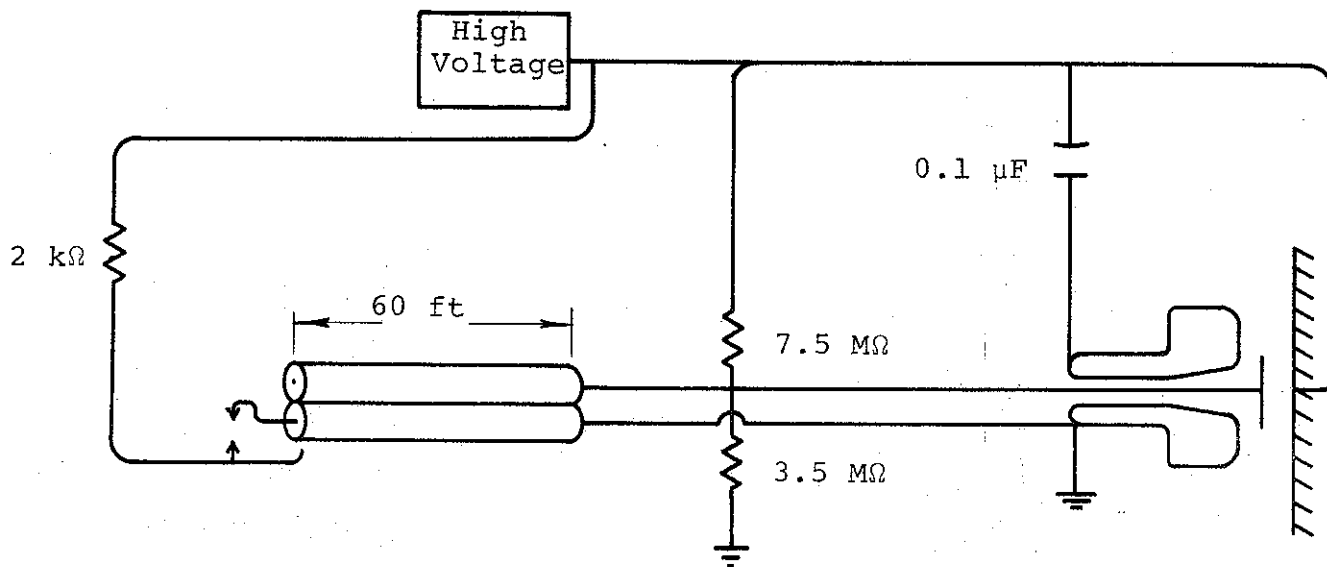


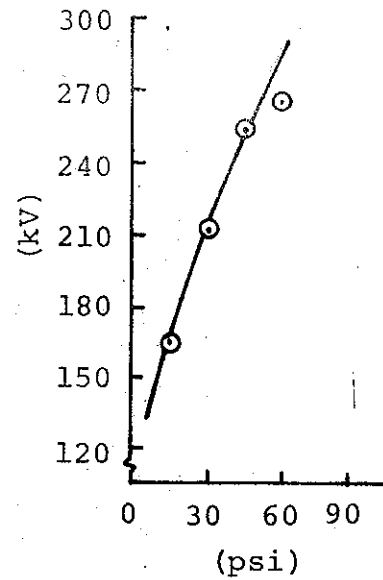
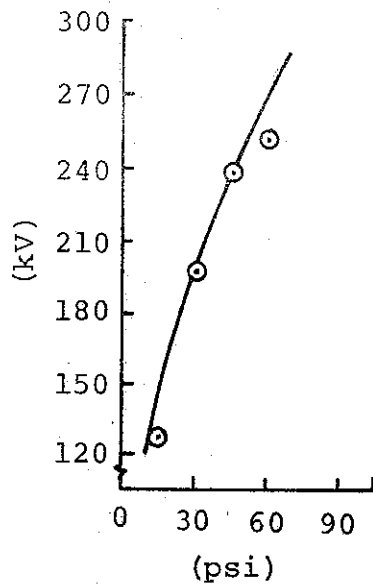
FIGURE 18. EXPERIMENT USING BLUMLEIN TRIGGER

were initially compared. The one with the smaller radius of curvature had a significantly lower self-breakdown voltage and was used in only one further test.

Figure 19 shows the self-breakdown behavior of the larger switch both dc and pulse charged. The dc self-fire strength of the switch at one atmosphere was ≈ 80 kV and seemed to scale in proportion to the gas pressure. However, this was less true at the higher pulse-charged levels; this may indicate that the trigger electrode potential was still not ideal. For instance, at 30 psig the self-breakdown voltage was 210 kV, while at 45 psig it was 252 kV. By taking the absolute pressures and setting up a proportion between them, the self-breakdown voltage at 60 psig would be expected to be 280 kV or 28 kV more than measured.

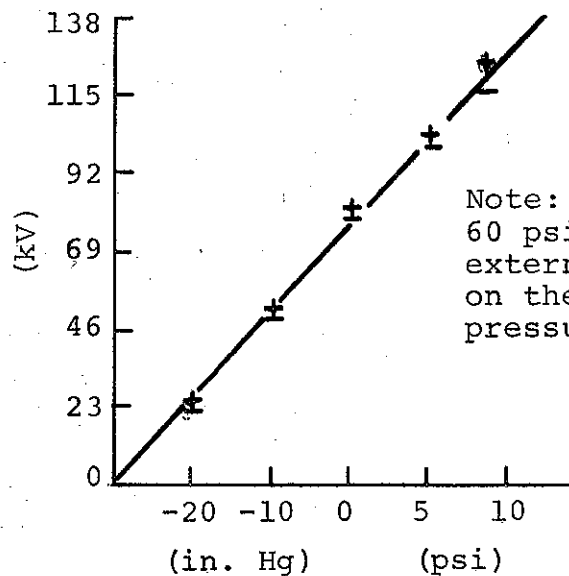
2. Triggering Range

With the experiment set up as in Figure 18, the dc voltage across the switch and on the Blumlein are the same. At atmospheric pressure in the first prototype, the minimum voltage at which the switch would fire was -17 kV ($\leq 25\%$ of self-fire), although not consistently. To ensure consistent firing, -19 kV was needed across the full gap of the three-electrode switch. The second prototype behaved similarly (Table II). At -19 kV the blumlein delivers a trigger of ≈ 32 kV to the middle electrode.



a. Gap Pressure Versus Pulse-Breakdown Voltage with a $\frac{2.8 \text{ k}\Omega}{5.4 \text{ k}\Omega}$ Resistive Divider

b. Gap Pressure Versus Pulse-Breakdown Voltage with a $\frac{550\Omega}{1000\Omega}$ Resistive Divider



Note: Data taken at 60 psi may be inaccurate; external tracking appeared on the insulator at this pressure.

c. Gap Pressure Versus dc Breakdown Voltage with a $\frac{4.5 \text{ M}\Omega}{7.5 \text{ M}\Omega}$ Resistive Divider

5260

FIGURE 19. SELF-BREAKDOWN STRENGTH OF SF₆ SWITCH--dc AND PULSED

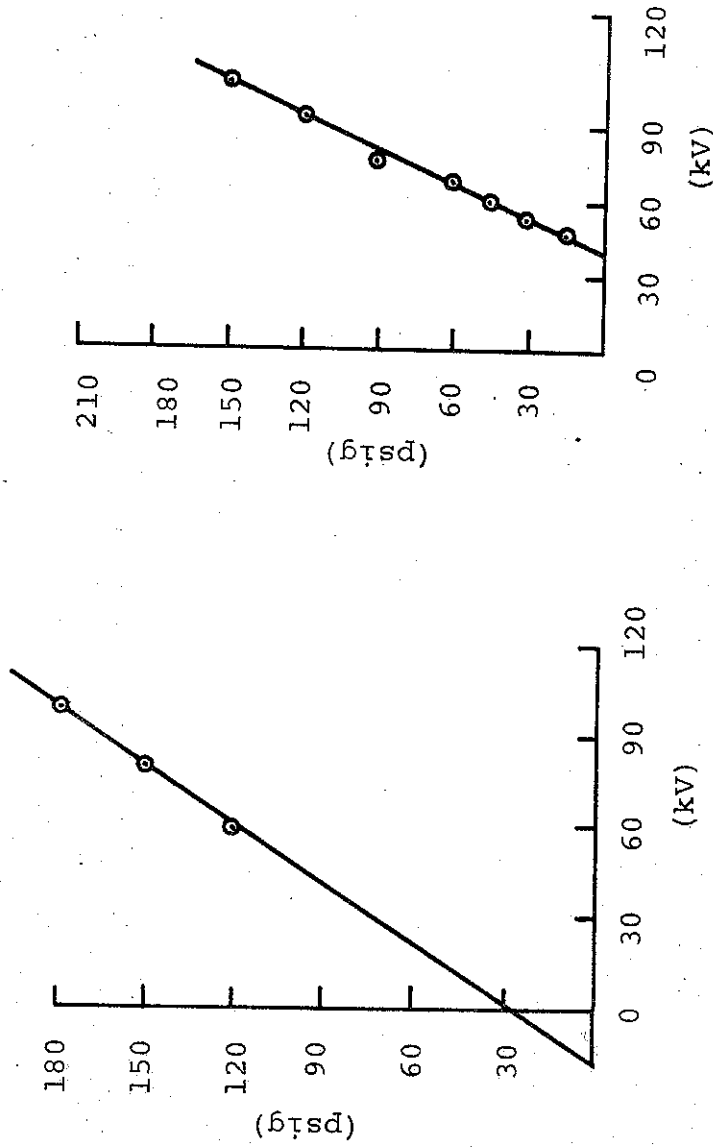
TABLE II

MINIMUM VOLTAGE REQUIRED TO FIRE WITH BLUMLEIN TRIGGER

<u>Voltage (kV)</u>	<u>Pressure of SF₆ (atm absolute)</u>
-21	1
+19	1
-30	2
+38	2
-18	2/3
+14	2/3

Further experiments relevant to the triggering range were conducted with an independent trigger source rather than the Blumlein trigger. Figure 20 presents the minimum trigger pulse voltage that would cause firing of the middle electrode of the switch to the dc charged electrode. The total potential across the gap was 52 kV plus the trigger voltage, since the trigger voltage was positive.

Next, the dc charge was removed from the switch and the trigger pulse was again applied, except now the gap that broke was from the middle electrode to the ground side, since it is the smaller gap (Figure 20b). For example, suppose the switch were pressurized to 45 psi. As Figure 20b illustrates, 45 psig corresponds to 60 kV; thus, at least ≈ 60 kV is needed across the switch if the smaller gap is to break after the middle electrode has broken the larger gap and the range of the switch is limited to voltages greater than 60 kV at 45 psig. Figure 19a indicates that at 45 psig the switch may be charged to 240 kV before self-breakdown, yielding approximately a 4:1 overall range



- a. Gap Pressure Versus Minimum Trigger Voltage Required to Fire Larger gap of Switch with -52 kV dc across Entire Switch
- b. Gap Pressure Versus Minimum Trigger Voltage Required to Fire Small Side of Switch with no dc Field across Entire Switch

FIGURE 20. MINIMUM TRIGGER VOLTAGE REQUIRED TO FIRE EITHER SIDE OF SWITCH

at 45 psig. Figure 20a may be used to get a rough approximation of the minimum trigger pulse required. At 45 psig the trigger pulse had to bring the potential difference to 62 kV (+10 kV and -52 kV) to fire the switch. Similarly, we can say with -60 kV across the switch, the trigger pulse would have to be very roughly +2 kV to fire the switch.

3. Jitter Measurements

The first measurements of switch jitter were taken with the configuration represented in Figure 18. At 25 kV dc across the switch and one atmosphere of SF₆, five shots were taken with each polarity. Figure 21 contains reproductions of oscilloscope traces of the middle electrode monitor. The middle electrode first swings with the trigger voltage, then to the overall voltage when the gap breaks to the high-voltage side. Finally, switching is completed when the middle electrode swings back toward ground. The jitter was estimated to be approximately 10 nsec.

It is of great advantage to utilize such a great sensitivity to trigger voltage because a portion of the voltage is lost through resistive division between 250 ohms in the trigger line and the balancing resistance of the resistors to ground.

The next jitter measurements were made using the experimental configuration of Figure 22. The results, some of which include the jitter of the isolating gap, are presented in Table III. It is estimated that the jitter in the isolating gap is approximately 2 to 4 nsec.



20 nsec
~45 kV/cm

a. + 25 kV Charge



20 nsec
~45 kV/cm

b. - 25 kV Charge

FIGURE 21. TRIGGER ELECTRODE WAVEFORMS

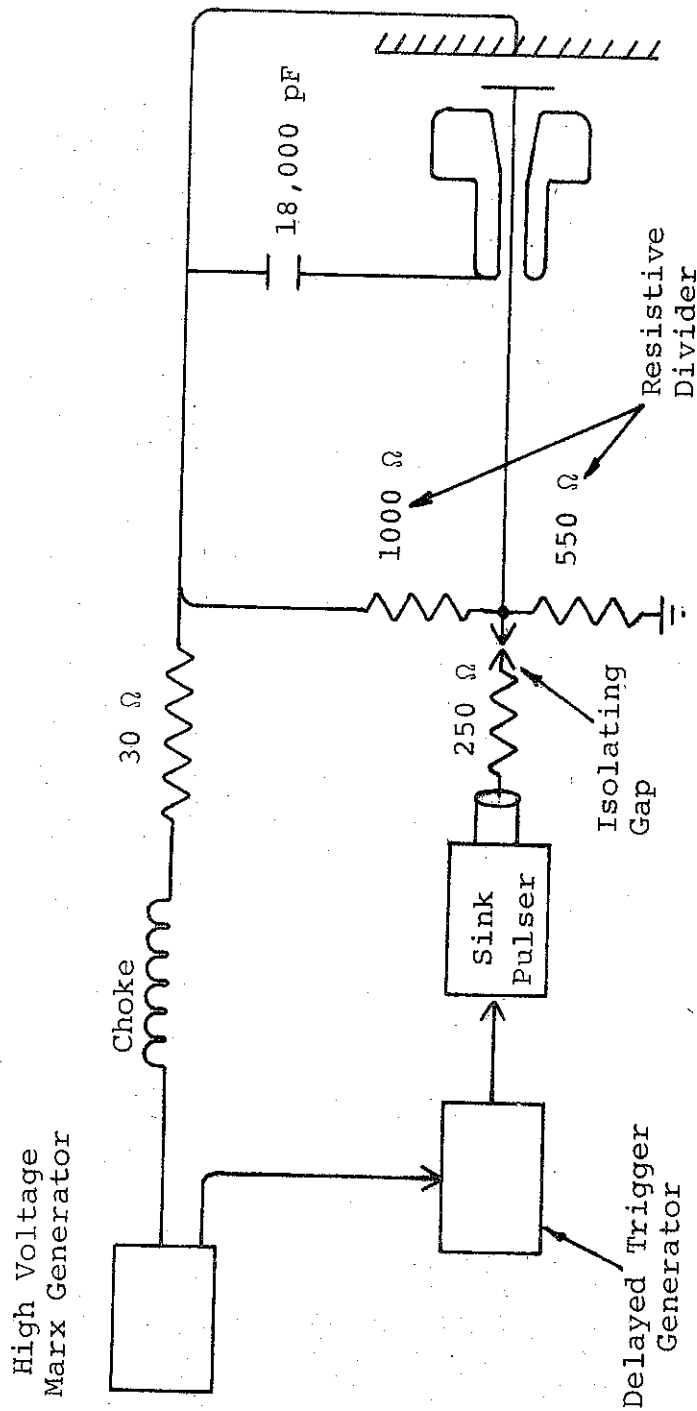


FIGURE 22. TEST ARRANGEMENT EMPLOYING AN INDEPENDENT TRIGGER SOURCE AND BALANCING RESISTIVE DIVIDER

TABLE III
AVERAGE JITTER AT DIFFERENT SWITCH PRESSURES

SF ₆	Pressure (psi)	Trigger Voltage (kV)	% of Self-Breakdown		Average Deviation of Delay (nsec)
			Lower Value Resistive Divider (See Figure 4b)	Higher-Value Resistive Divider (See Figure 4a)	
	30	-60		87	2
	30	-80		80	40
	35	-68	80		16*
	40	-60	86		18*
	45	-60		82	5
	45	-80		72	3
	50	-68	72		12*
	60	-60	78		11*
	60	-60		73	unknown**
	60	-60		68	6
	60	-80	73		7*
	60	-80		67	5
	60	-100	70		24*

*Includes jitter of small isolating gap

**Of the four measured points of switch closure on this shot, three were within 30 nsec average jitter, but the fourth failed to trigger within the sweep of the oscilloscope.

In the next experiment, the three-electrode switch was pulse charged to higher voltages. Table IV presents the switch jitter calculated as the average deviation in the delay between application of trigger pulse and closure of the three-electrode switch. The jitter is given at different pressures and trigger voltages and is compiled from four consecutive shots at each setting. Possibly a degree of jitter is added because the condition of the gas from shot to shot is not completely controlled. This problem would not exist with simultaneous multiple switching (with switches sharing a common gas supply).

The jitter is clearly a function of overall voltage as well as trigger voltage. As the overall voltage approaches self-breakdown, jitter decreases. It would be impractical to run the switches very near self-breakdown because the probability of self-fire increases greatly near the self-breakdown threshold. It was suspected that some of the data in Table IV included some self-breakdown, which increased jitter considerably. There were none in Table V, however.

From Table IV a predictive graph of jitter for the prototype switch was constructed (Figure 23). The shots were taken with a positive overall voltage and a negative trigger voltage. Later experiments indicate the best polarity for a V/3 switch is negative overall voltage for minimum jitter.

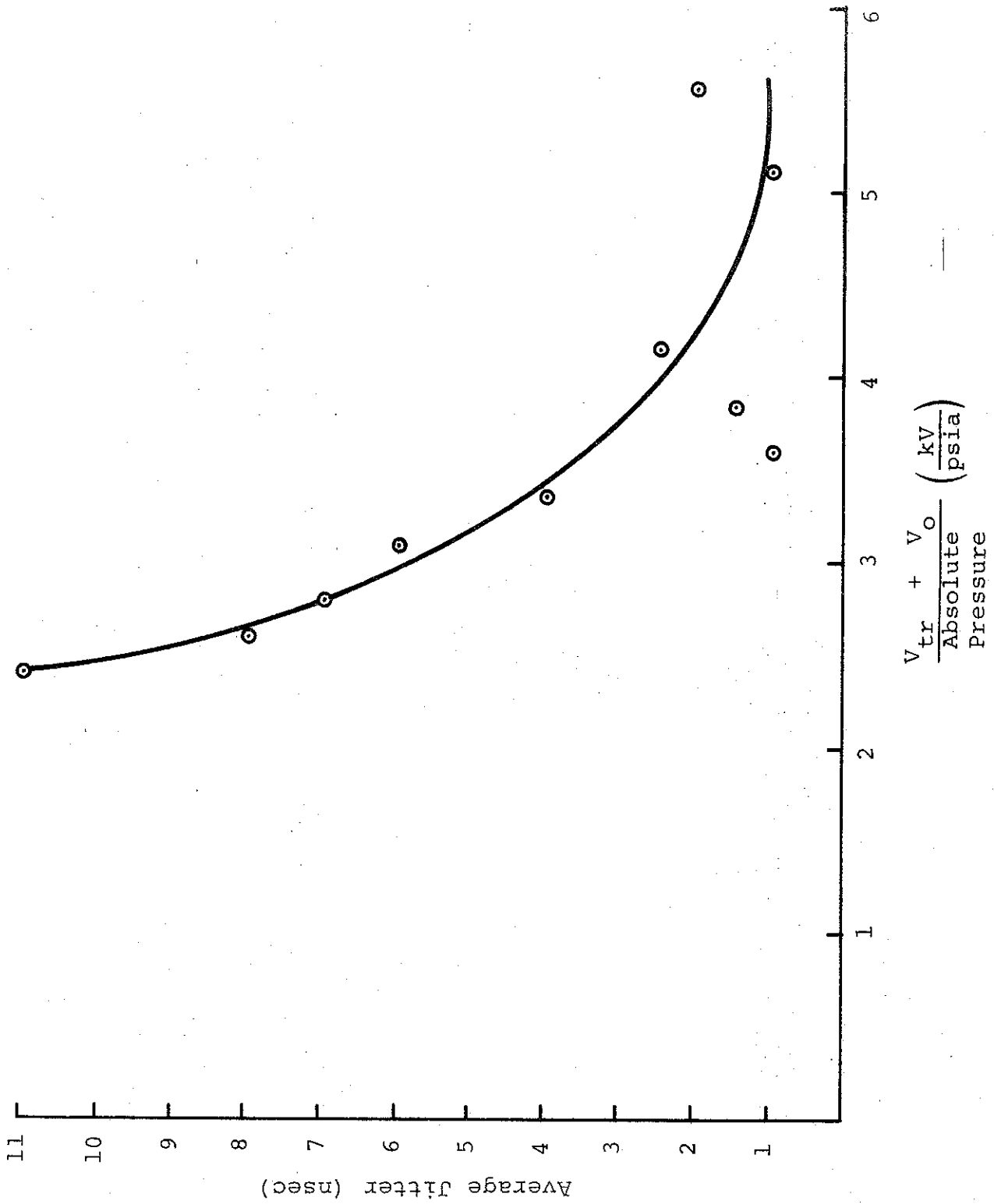


FIGURE 23. AVERAGE JITTER AS A FUNCTION OF TRIGGER AND OVERALL VOLTAGE COMPUTED FROM TABLE I

TABLE IV
 AVERAGE JITTER OF THE SWITCH
 UNDER VARIOUS CONDITIONS

<u>SF₆</u> <u>(psi)</u>	<u>Trigger</u> <u>(kV)</u>	<u>Overall Voltage</u> <u>(% of self-fire)</u>	<u>Overall</u> <u>Voltage</u> <u>(kV)</u>	<u>Delay</u> <u>(nsec)</u>	<u>Deviation</u> <u>of Delay</u> <u>(nsec)</u>
30	-60	81	170	70	1
	-80	81	170	65	2
45	-60	68	170	100	1.5
	-80	68	170	100	2.5
60	-60	55	170	140	6
	-80	55	170	140	4
	-100	55	170	160	1
90	-80	54	195	250	8
	-80	70	250	180	6.5
	-100	54	195	300	7
120	-80	62	250	240	11
	-100	62	250	220	8

Since the trigger pulse is the opposite polarity of the overall voltage, the actual potential drop between the middle electrode and the high voltage side (the larger gap) is equal in magnitude to $|V_{tr}| + |V_o|$. As the ratio between this value and the pressure decreases the average jitter measured decreases. The larger gap contributes the main portion of the jitter. In the opposite set of polarities, main jitter occurs in switching the smaller gap; then the ratio of V_o to the pressure controls the jitters. The graph should be taken as only a rough approximation because the other factors influence jitters.

The jitter does not continually decrease by raising the trigger voltage V_{tr} . At too high a trigger the smaller gap breaks first and the final closure of the switch occurs much later, with a greatly increased jitter. In the particular switch used during the experiment the maximum trigger applied could not be more than approximately 70% of V_o in magnitude without increasing the jitter.

It is important to note that the polarity of the experiment from which Figure 23 and Table IV were drawn was a positive overall voltage and a negative trigger pulse. Other polarities would have given different results, as will be seen in the next section, but the general trends would most likely remain. The practical reason for the choice of polarities was that they would be compatible with the 2/3-ohm water generator.

4. Multiple Switching

Six SF₆ switches were installed in the 2/3-ohm water line. Access to the switches was difficult and their very installation was a lengthy process. Time permitted only preliminary trials and difficulties were encountered. In the first trial, the water line was pulse-charged to 120 kV and one switch broke at the lucite envelope,

which had been shortened to fit in the water line. Two more switches then broke at 80 kV. It was concluded that the water line should be specifically designed around the SF₆ switches to allow proper access for experimentation. The program schedule, however, did not permit the effort to be extended in order to conduct these experiments.

5. Conclusions

The first design for a high-voltage SF₆ switch was tested in a water environment with low jitter and voltages up to 250 kV. There was reason to believe that the voltage could be increased to 1 MV with the same low jitter. The results of this experiment pointed to ways of designing even higher-voltage switches with similar basic designs.

SECTION III

THREE-ELECTRODE, OPEN-TRANSMISSION-LINE FED, SF₆ SWITCH

After the experiments were completed with a three-electrode switch in water, further studies were made with three-electrode switches in an effort to develop the design to produce jitters a few nanoseconds or less in the 1 MV region. It was felt that an oil environment was suitable for low-jitter switching because the stray capacities of the switch that contribute to jitter could be most easily minimized, and because diagnostics would be facilitated.

Because of the similarities in the performance characteristics desired of the three-electrode switch in the trigatron contract and the switching requirements in SIEGE II, equipment was developed in the SIEGE II, Phase II, program that was appropriate for the present project. This equipment also served for many other tests in the SIEGE Program, and therefore delayed work in the present contract until the SIEGE II work was complete.

A. APPARATUS

1. Circuit

In the tests to be discussed a 14-1/2-stage Marx with an output capacity of approximately 2.6 nF was used. Although the Marx was capable of ringing up to over 2 MV, most of the tests were performed at around 1 MV because the tank size was inadequate for higher voltages.

Figure 24 is a schematic of the important components of the experiment. In Figure 24 the copper-sulfate monitor of the M-switch is represented by 4 kohms and a tapoff resistor;

8312

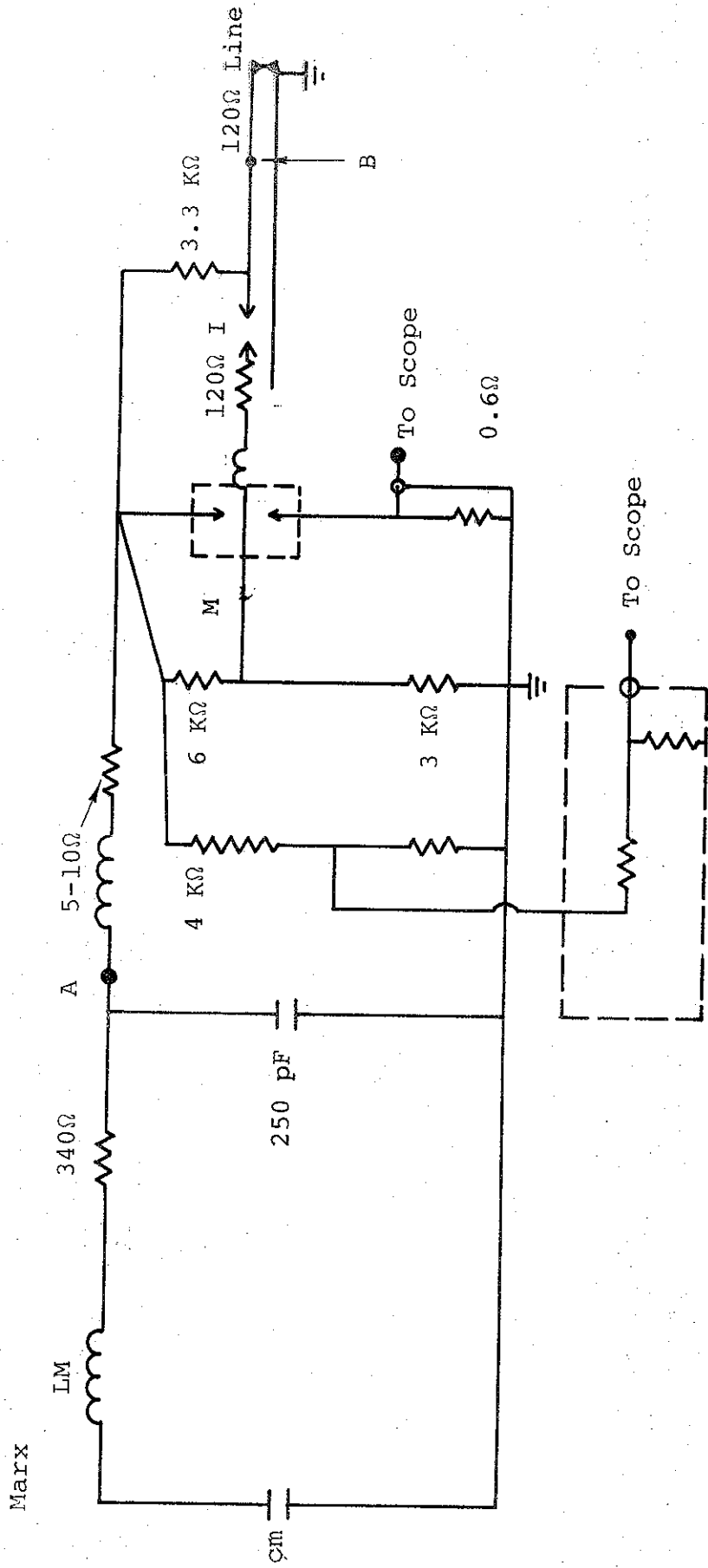


FIGURE 24. EXPERIMENTAL CIRCUIT

the current monitor by 0.6 ohms.

The Marx is represented by CM and LM. It charges a parallel-plate oil capacitor through 340 ohms. The capacitor is connected to the three-electrode switch under test (the M-switch) through a 5- to 10-ohm resistor. The Marx also charges the 120-ohm trigger transmission line through an additional 3.3 kohm. The trigger line is switched by the spark gap S. Because of the capacity of the 10-ft, 120-ohm trigger line and the additional resistance, the risetime across S is slower than across M.

As the voltage rises on M, the balancing resistors, 6 kohm and 3 kohm, keep the middle electrode at 1/3 the overall potential V_0 . (In the case of an M-switch with midplane electrode, 4 kohm and 4 kohm were used.) The function of the I-gap was to isolate the middle electrode from the trigger-line voltage during pulse charge.

2. Switches

The first M-switch tested is sketched in Figure 25 and a photograph of it appears in Figure 26. Most of the SIEGE II testing was performed using this switch; however, for the trigatron contract it was decided to lengthen the envelope to 10 in. (Figure 27) because trigger pulses had a tendency to cause tracking on the gas-lucite interface. Because it was desirable to minimize the stray capacity of the middle electrode, the part that extends between the lucite sections was cut off and the middle electrode held in place by only three 1/4-in.-diameter rods through the tubing. Since the middle electrode was normally at V/3 potential, the switch was referred to as the V/3 M-switch.

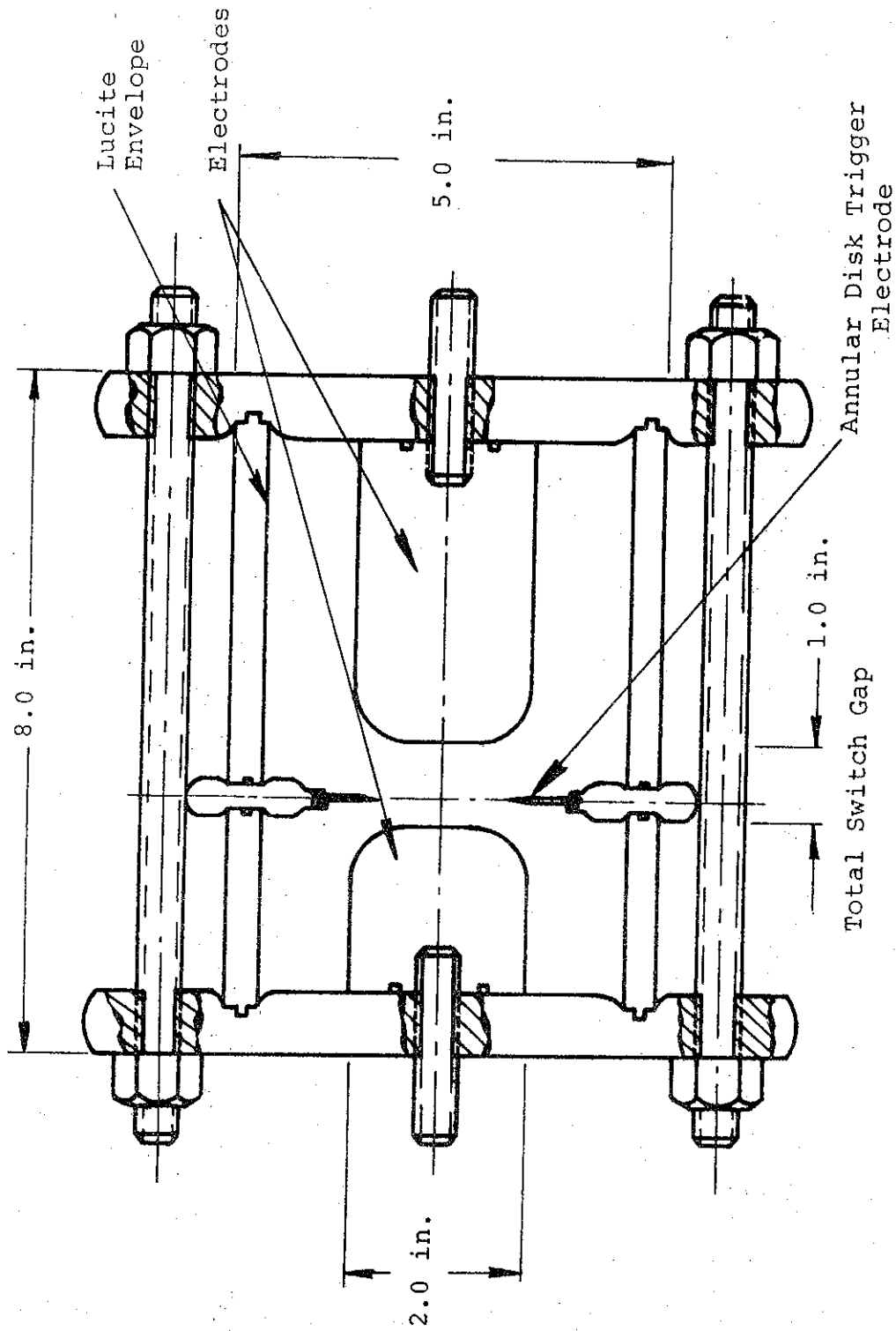


FIGURE 25. THREE-ELECTRODE SF₆ SWITCH (FIRST CONFIGURATION)

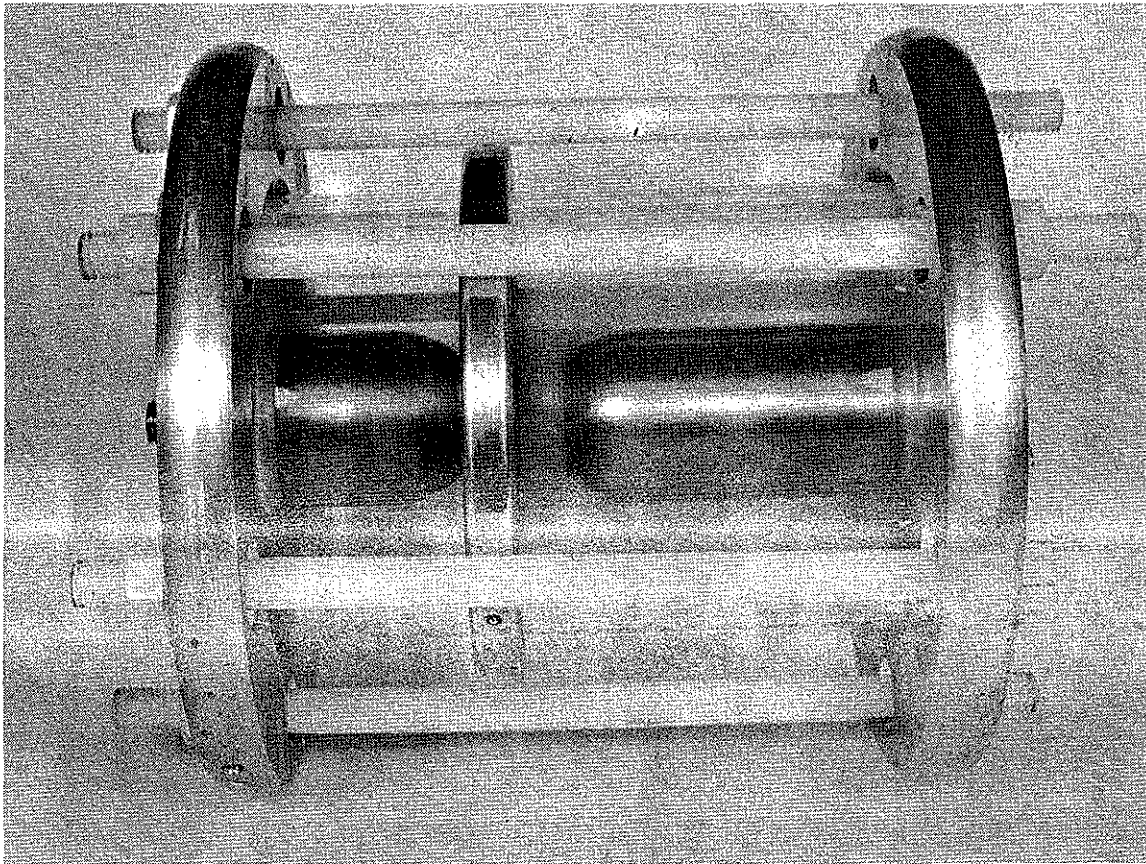


FIGURE 26. THREE-ELECTRODE SF₆ SWITCH,
(FIRST CONFIGURATION)

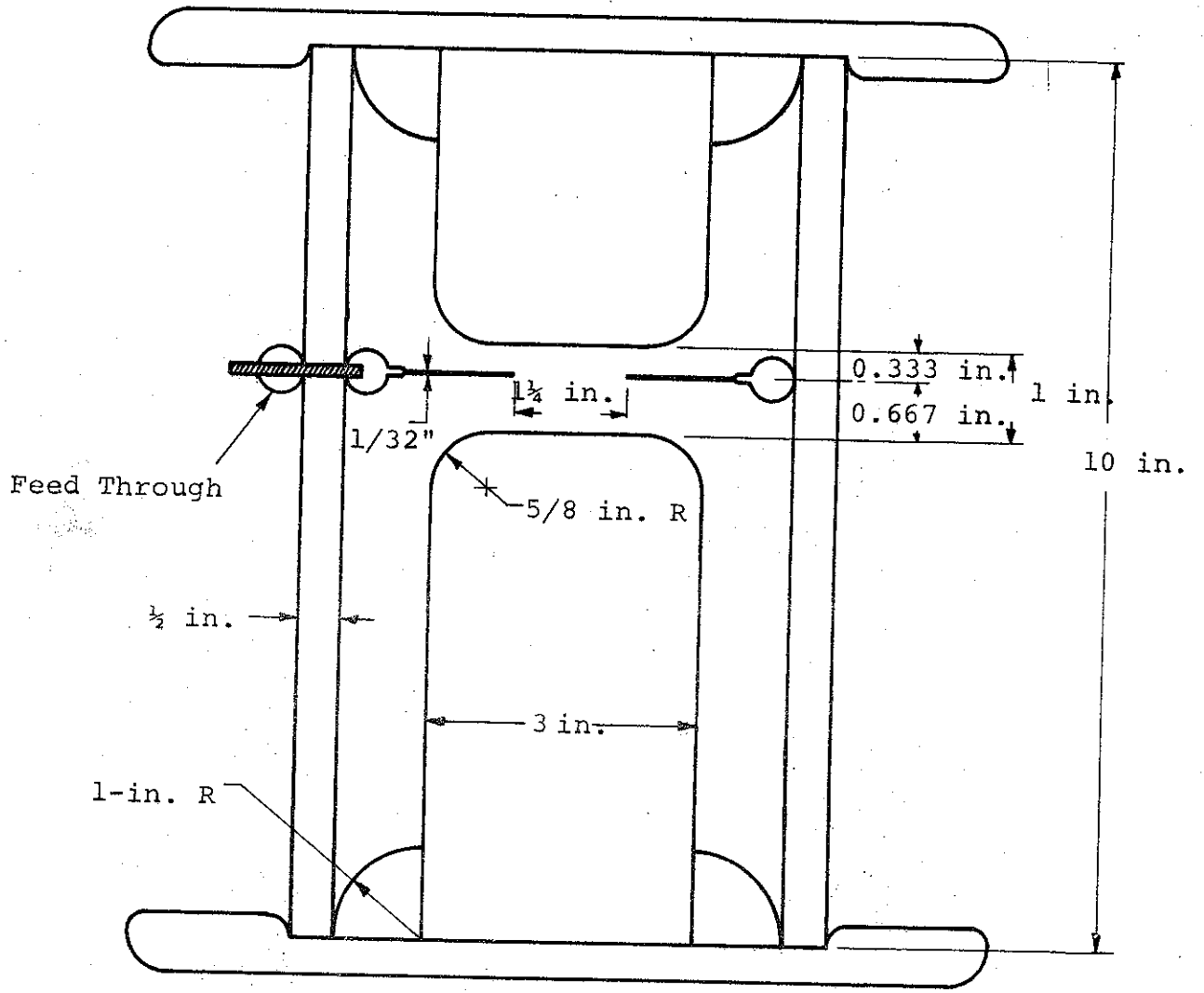


FIGURE 27. THREE ELECTRODE SF₆ SWITCH--SECOND CONFIGURATION

8580

The same type of middle electrode was placed in the V/2 position in another switch called the V/2 switch. There was only enough lucite on hand for a 7-in. envelope. The same 7-in. lucite envelope was also employed to make a V/2 "wiretype" M-switch in which the middle electrode was a 23-mil-diameter stainless-steel wire stretched across the center of the gap.

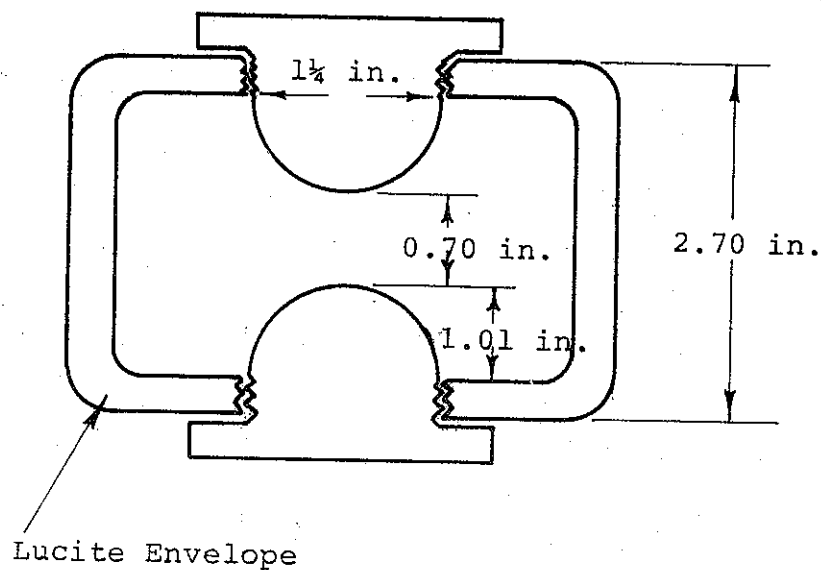
In all the above mentioned switches it was possible to use another set of outer electrodes with a 3-in. o.d. They were exactly the same length as the smaller electrodes, but because of their larger size they produce a more uniform field and, hence, a larger field near the trigger electrode.

3. Accessory Gaps

Two accessory gaps were used: one to supply the trigger pulse and the other as an isolating gap. The S-gap was a small, uniform-field, self-breaking switch (Figure 28). The S-gap and the isolation gap were both electrically symmetrical (Figure 29). The I-gap was built long and narrow and placed on the end of the trigger line so that it would appear as a continuation of the transmission-line ($Z = 120$ ohms) cylinder over ground plane and give rise to minimal reflection when conducting. Pressure in all three spark gaps was externally controlled.

4. Monitors

A fast copper-sulfate monitor was used to measure the overall voltage immediately across the three-electrode switch. It was built to fit compactly between the end plates of the switch so that the capacitive division was in the same ratio as the resistive one, making for an accurate and fast monitor (Figure 30).



Spacing, 0.70 in. = 1.78 cm
Radius (ball electrodes) = 1.58 cm

FIGURE 28. UNIFORM FIELD GAP

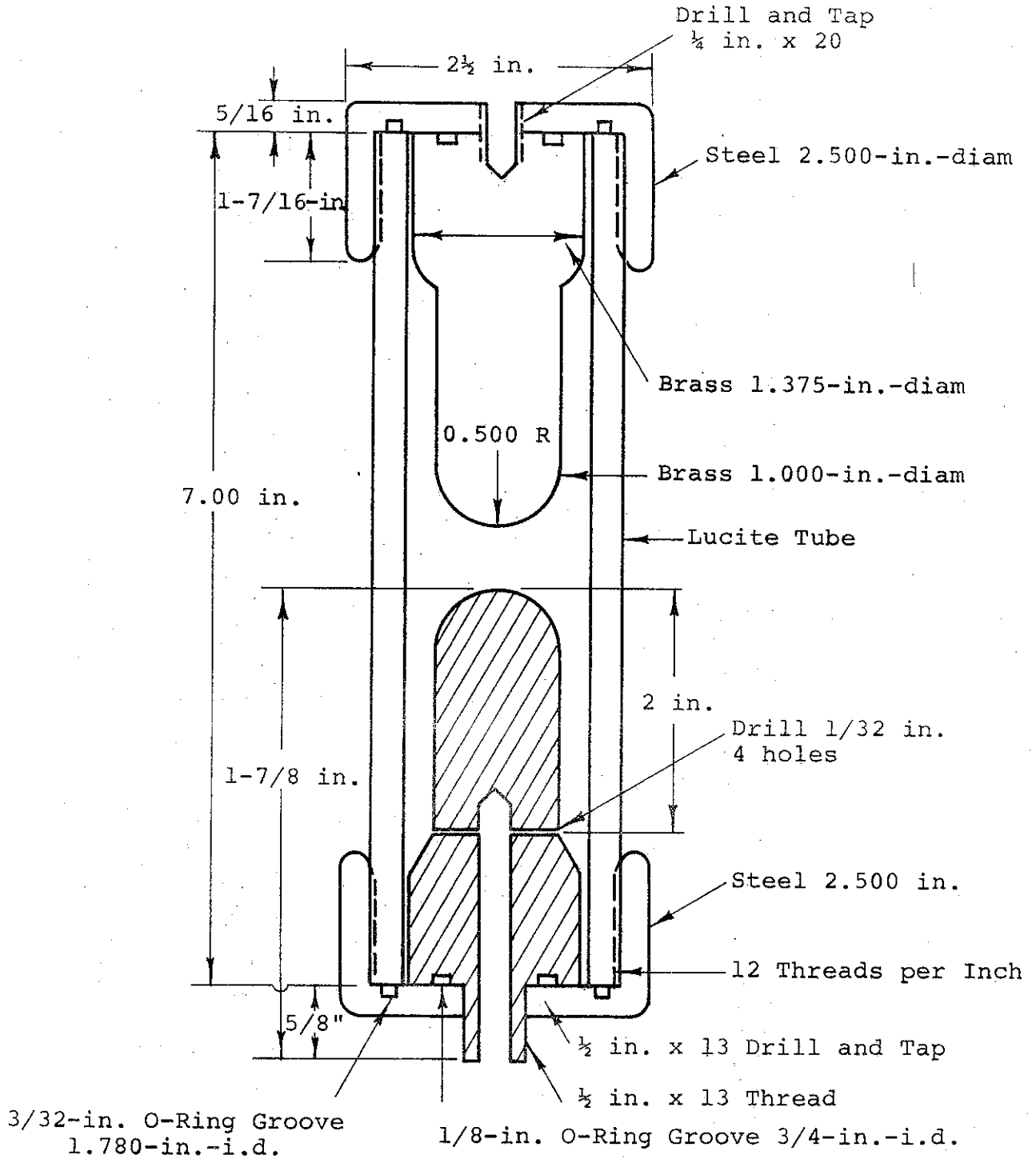
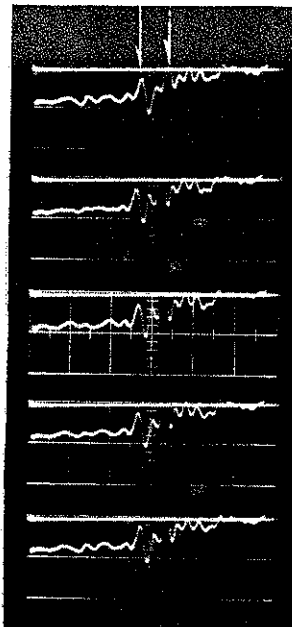


FIGURE 29. I GAP

1 2



10 nsec/cm

- 1 - First Part of M Switch Fires
- 2 - Second Part of M Switch Fires

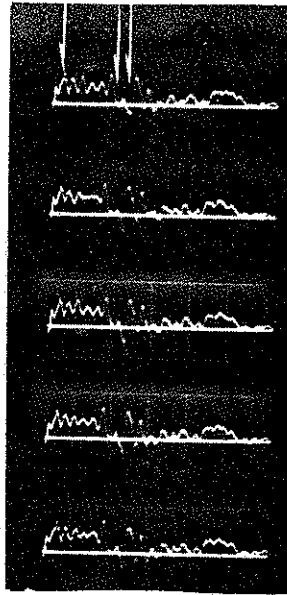
FIGURE 30. VOLTAGE TRACES FROM FAST CuSO_4 MONITOR

The trigger pulse was generated in a transmission line formed by a 1-in. pipe, 5-1/2-in. above a ground plane. A copper-sulfate monitor could not be used to monitor the pulse because the spacing was too small. Instead, an E-field monitor, basically a capacitive divider, was placed in the line just ahead of the I-gap. The E-field monitor was formed by placing a small flat plate (roughly 3 in. x 9 in.) on a 1/32-in. polyethylene sheet on the ground plane, under and across the transmission line. One-hundred ohms in series with the 500 pF of the monitor limited the signal decay so that pulses up to 25 nsec long would not be noticeably distorted. Signals from the E-field monitor (Figure 31) displayed the rise of the trigger pulse and its reflection from the I-gap, the breakdown of the I-gap, and the firing of both parts of the three-electrode switch.

No attempt was made to measure the absolute amplitude of the trigger pulse with the E-field monitor. Because the trigger pulse is generated by the closure of a switch, S, after the line has been pulse-charged, it is only necessary to measure the pulse-charge voltage to determine the trigger-pulse amplitude. A copper-sulfate monitor attached across the S-gap measured its pulse charge, $\pm V_{tr}$, indicating a trigger pulse $+V_{tr}$, since the line ends in an open circuit at the middle electrode. This copper sulfate monitor was fairly slow in response and could not give the accurate waveshape of the trigger pulse.

The fourth monitor was a ring of carbon resistors in series with the base of the three-electrode switch and the ground plane. The resistors had a parallel value of approximately 1/2 ohm. As current passed through these carbon resistors a signal of 500 V/kA was sent into the 50-ohm cable connected to the bottom of the switch through a hole in the ground plane. The current monitor

1 23



10 nsec/cm

- 1 - I Gap Fires
- 2 - First Part of M Switch Fires
- 3 - Second Part of M Switch Fires

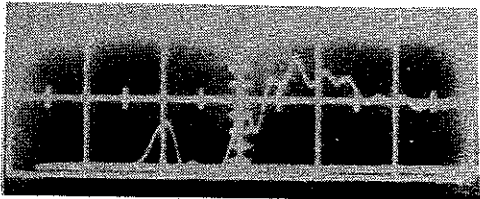
FIGURE 31. E-FIELD MONITOR VOLTAGE TRACE

complemented the copper sulfate monitor in that they both measured the closure times of the top half and bottom half of the three-electrode switch (Figure 32).

5. Sequence of Circuit Operation

Fast pulse events begin when the S-gap fires. Since the trigger-line pulse charge is only one-tenth as fast as M (Figure 33), the latter is fully charged to V_0 when S fires. Hence, varying the amplitude at which S fires conveniently leaves the voltage on M unchanged. This produces a pulse with a 10 to 90% risetime of about 1-1/2 nsec, which eventually appears as \bar{V}_{tr} across the I-gap. The risetime of the ≤ 1 -pF capacity of the I-switch charging through the transmission line on the right, and its continuation through a 120-ohm resistor on the left, will add only about 0.4 nsec (10 to 90%). The I-gap is adjusted to its minimum safe working pressure to minimize the jitter associated with its closure. Due to capacitive coupling (Figure 34), a small prepulse of less than one-sixth the trigger voltage precedes the breaking of the I-gap. Once the I gap has broken, the voltage on the middle electrode will begin to change from $\pm 1/3 V_0$ (or $\pm 1/2 V_0$ in the wire type) to approximately \bar{V}_{tr} with a time characteristic of an RCL circuit.

The middle electrode never reaches \bar{V}_{tr} because the impedance driving it (240 ohms) is comparable in size to the impedance of the resistive divider trying to keep it in place. The resulting resistive division allows only $\mp 0.9 V_{tr}$. The duration of the trigger pulse is 25 nsec.



6 kA/cm

5 nsec/cm

$V_o = +460$ kV

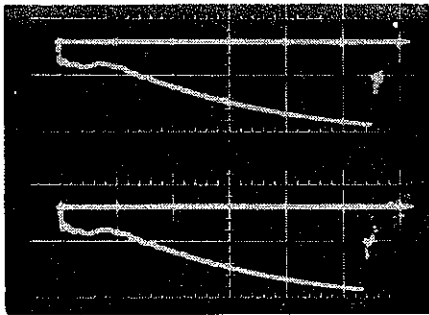
$2V_{tr} = -500$ kV



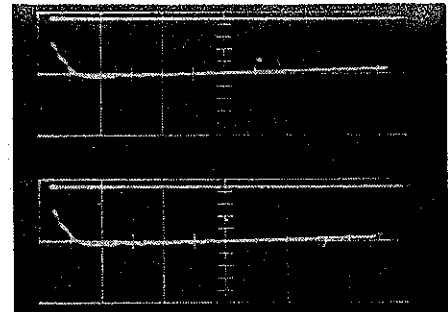
(1) First Part of M Discharges

(2) Second Part of M Discharges

FIGURE 32. CURRENT MONITOR



S-gap voltage, 400 kV/cm
200 nsec/cm



M-gap voltage, 900 kV/cm
200 nsec/cm

FIGURE 33. S- AND M-GAP VOLTAGE WAVEFORMS

7715

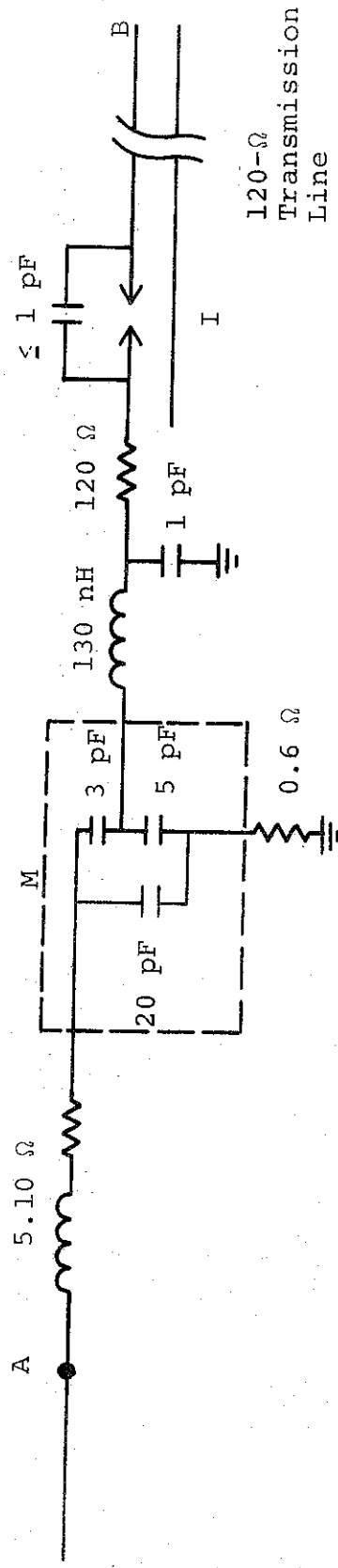


FIGURE 34. EXPERIMENTAL CIRCUIT DETAIL

Figure 32 is the oscilloscope trace used to estimate the capacitance to ground of the middle electrode. The triangular-shaped pulse before the main current surge represents the breakdown of half of switch M; the main surge indicates complete closure. The integral of the triangle gives the charge difference when the capacitance goes from $\mp 0.9 V_{tr}$ to $\pm V_o$. The ratio Q/V yields 5 pF, which is close to the estimate arrived at geometrically. The capacity of the high-voltage electrode to the trigger electrode will be somewhat less, about 3 pF.

Thus, the RCL circuit ($R = 240 \Omega$, $C = 8 \text{ pF}$, $L = 130 \text{ nH}$) is barely underdamped, and the middle electrode will change its potential from $\pm V_o/3$ to approximately $\mp V_{tr}$ in about 2 nsec. Before the end of the 25 nsec trigger pulse the top half of M will usually break and the middle electrode will begin to change from $\mp 0.9 V_{tr}$ to some voltage near $\pm V_o$.

At this point the importance of the impedance holding the overall voltage on M-switch becomes apparent. As illustrated in Figures 24 and 34, a 5- to 10-ohm resistor was used between the 250-pF capacitor and the M-switch. If there was an open circuit the trigger pulse would tend to discharge the initial overall voltage on M. However, the recharging time of the approximately 22-pF stray capacity through 10 ohms is only approximately 0.2 nsec, much less than the risetime of the trigger pulse. With an 80-ohm resistance used in initial testing, the time constant is approximately 1.8 nsec and thus comparable to the risetime. Also, the resistive division between 80 ohms and 240 ohms (trigger line and trigger resistor) allows only $\pm 3/4 V_o$ to be applied to trigger electrode to break the second side of the switch. Evidence in this border line case indicated low jitters were still possible. Finally, a 240-ohm resistor was tried and the resulting jitter was quite high.

If there is a long delay (approximately 25 nsec) in firing the second part of M, the trigger line will no longer look like 120 ohms but 0 ohms, and the resistive division would be between an 80 ohms and the 120-ohm resistor. Also the 250-pF capacitor discharges in 60 nsec into the trigger line. However, this generally is not the case since the second part usually fires as promptly.

Delay and jitter are measured by using the closure of the S-gap or the E-field probe signal to trigger a scope or scopes displaying the M-gap voltage, the M-gap current, or the E-field probe itself; sometimes all of these signals were recorded.

B. RESULTS

1. Trigger Pulse vs S-Gap Pressure

In the following pages the pressure for S is given for each experiment. Using Figure 35, the actual voltage at which the trigger line discharged can be determined. Where the trigger line ended in an open circuit, $-V_{tr}$ would be seen at the open end, but as explained in the section on circuit analysis the trigger voltage is roughly $-0.9 V_{tr}$.

2. Pressure Dependence of M-Switch

In Figure 36, a and b, a scan of five pressure in the V/3 switch with 2 in.-diam electrodes yields the dependence of overall delay and jitter on gap pressure, at -1.25 MV. The gap self-fired at approximately 75 psig, and since the jitter curve was nearly level at 90 psig it was not felt much would be gained by more closely approaching the self-fire pressure. In Table V the data from which Figure 36, a and b, were drawn is tabulated. In the second column is displayed the delay and jitter for the first part of the switch to fire; the third column is the second part of the firing (middle electrode to ground electrode); and the fourth column is for the combination. The jitter and delay due to the I-gap were excluded.

Table VI differs from Table V in that 3-in.-diameter outer electrodes were used in the M switch. All other parameters were the same. The larger diameter electrodes were tried because they put the V/3 middle electrode deeper into the high uniform-field region. The performance at high pressures was thereby improved but at low pressures this improvement probably was counteracted by increased trigger-electrode capacity (Figure 37).

In Table VII a higher trigger voltage was used than in Table V.

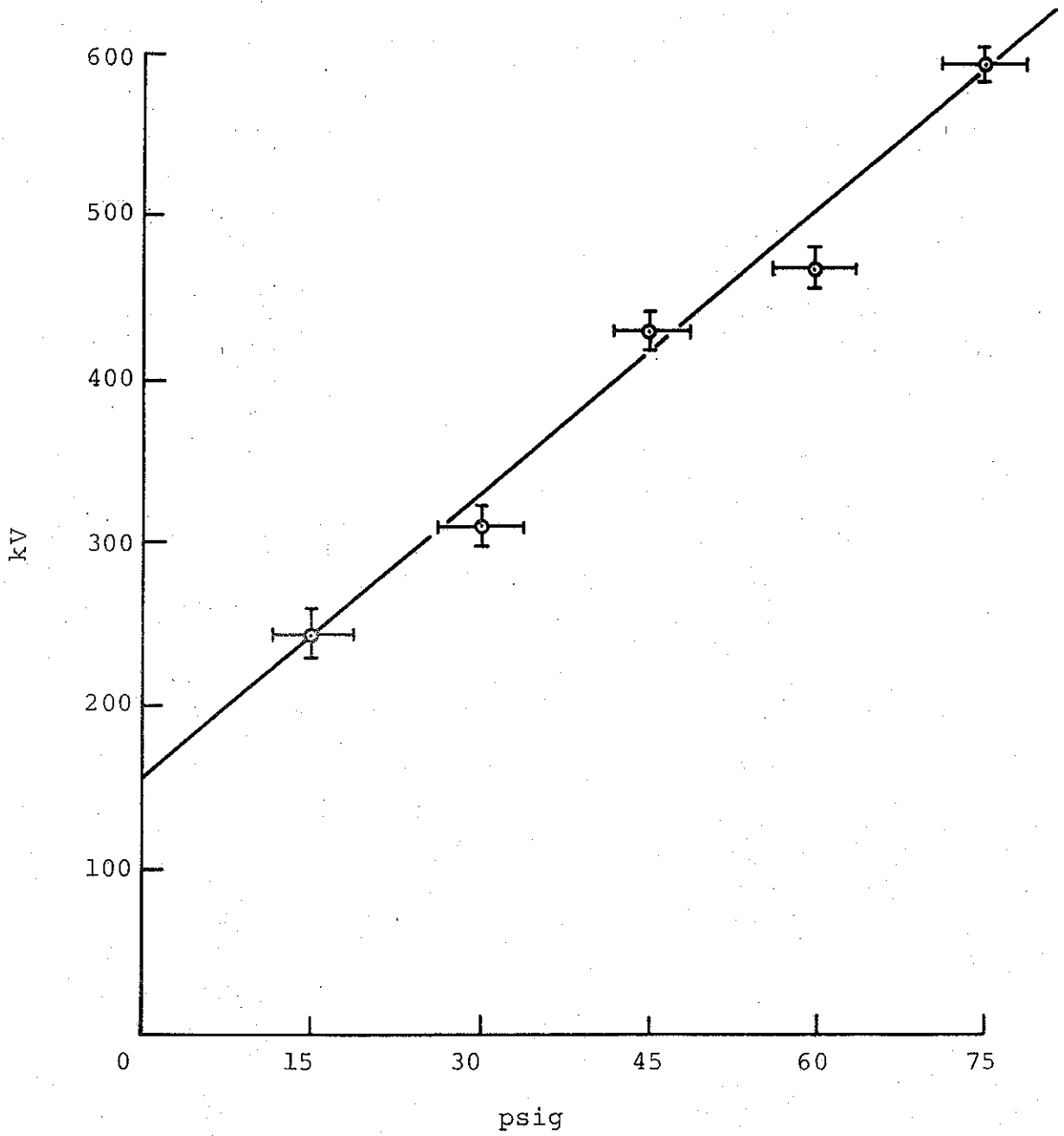
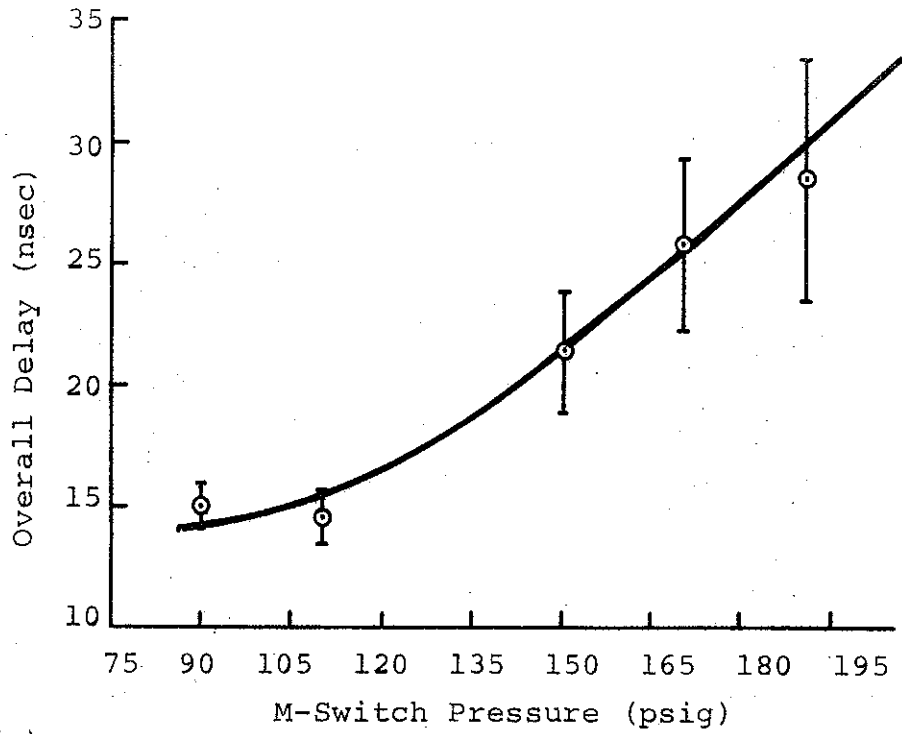
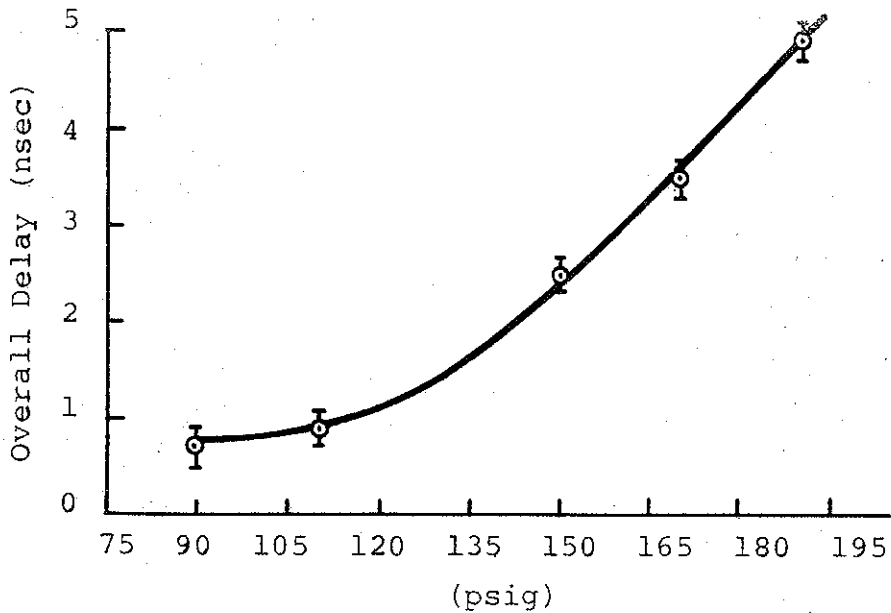


FIGURE 35. S GAP PRESSURE VERSUS BREAKDOWN VOLTAGE

7600



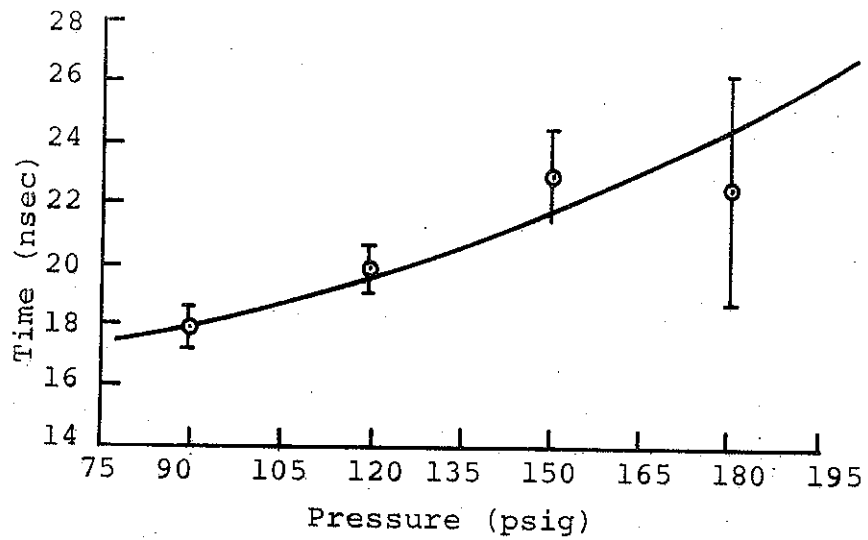
(a) Delay--Error Bars = \pm Jitter



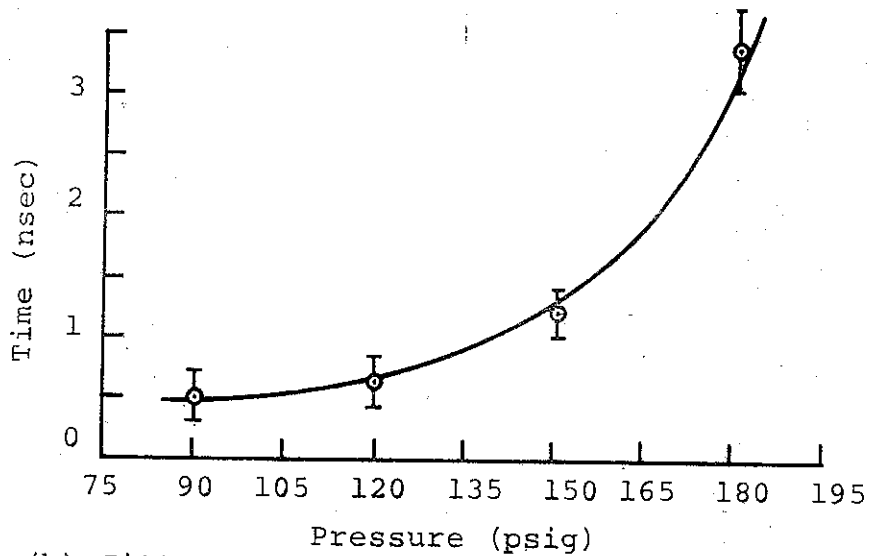
(b) Jitter--Error Bars = Measurement Error

8582

FIGURE 36. OVERALL DELAY AND JITTER OF V/3 M-SWITCH VERSUS PRESSURE (2-in. diam Electrodes, -1.25 MV)



(a) Delay--Error Bars=Jitter



(b) Jitter--Error Bars=Measurement Errors

FIGURE 37. V/3 M-SWITCH OVERALL DELAY AND JITTER
(3-in.-diam Electrodes, -1.25 MV)

TABLE V

M, S, I, (psig)	delay ₁ ± jitter ₁ (nsec)	delay ₂ ± jitter	delay _o ± jitter _o (overall)
-----------------	--	-----------------------------	---

90, 40, 20	9.8 ± 0.44	5.2 ± 0.38	15.0 ± 0.76
110, 40, 20	9.5 ± 0.62	5.1 ± 0.29	14.5 ± 0.92
150, 40, 20	10.6 ± 0.97	10.9 ± 2.28	21.4 ± 2.48
170, 40, 20	11.4 ± 0.72	14.7 ± 3.07	26.1 ± 3.46
190, 40, 20	12.1 ± 0.99	16.6 ± 5.41	28.7 ± 4.93

V/3 M switch with 2-in.-diam electrodes, pulse charged to -1.25 MV.

TABLE VI

90, 40, 20	11.5 ± 0.45	6.5 ± 0.38	18.0 ± 0.57
120, 40, 20	12.4 ± 0.46	8.0 ± 0.40	20.4 ± 0.71
150, 40, 20	13.5 ± 0.79	9.6 ± 0.79	23.1 ± 1.44
180, 40, 20	13.3 ± 0.35	9.5 ± 4.25	22.7 ± 3.82

V/3 M switch with 3-in.-diam electrodes, pulse charged to -1.25 MV.

TABLE VII

90, 60, 35	9.7 ± 0.44	5.5 ± 0.49	15.2 ± 0.77
120, 60, 35	9.8 ± ----	9.7 ± 0.60	19.5 ± ---
150, 60, 35	-----	12.3 ± 3.79	---- ± 5.0
190, 60, 35	-----	14.9 ±	-----

V/3 M switch with 2-in.-diam electrodes, pulse charged to -1.25 MV, experimental error ± 0.25 nsec.

In Table VIII the same M-switch is used as in Table VI except at a lower voltage, -980 kV. When the voltage is reversed (+980 kV) (Table IX) the jitter increases (Figure 38). But for the V/2 M switch at an intermediate voltage, +1.1 MV (Table X), the positive polarity jitter drops back to the order of 1 nsec.

Table XI goes back to the conditions of Table VI, except the I-gap was removed and a 40 pF capacitor put in its place. Because of the absence of I-gap the M-switch self-fired occasionally at 90 psig. Apparently, even though no self-fires were considered in the averages, the closeness to self-fire was unfavorable to achieve low jitter. Had the capacitor been smaller, the balancing resistors may have been able to work more effectively, but then more of the trigger pulse would be reflected and not reach the middle electrode. The last three sets of shots were taken after some work in the Marx during which time the trigger line was disconnected and reconnected in a new way to reduce the inductance between trigger line and switch, thereby reducing jitter and delay in firing the first part of M.

3. Trigger Voltage Dependence of M-Switch

Tables V through XI are presented to show the dependence of delay and jitter on the pressure in M under various conditions. The effect of varying the trigger voltage was then explored.

TABLE VIII

M, S, I, (psig)	delay ₁ ± jitter ₁ (nsec)	delay ₂ ± jitter	delay ₀ ± jitter ₀ (overall)
75, 40, 20	11.9 ± 0.59	5.5 ± 0.00	17.1 ± 0.59
90, 40, 20	12.3	4.8	18.0
103, 40, 20	12.5 ± 0.47	9.6 ± 0.48	22.1 ± 0.62
120, 40, 20	14.6 ± 0.66	14.3 ± 3.19	18.9 ± 3.20
150, 40, 20	-----	18.5 ± 5.78	-----

V/3 M switch with 3-in.-diam electrodes, pulse charged to -980 kV
experimental error ± 0.40 nsec

TABLE IX

60, 40, 20	14.8 ± 2.58	3.5 ± 0.00	18.3 ± 2.58
75, 40, 20	18.2 ± 2.98	5.4 ± 0.01	23.3 ± 2.98
90, 40, 20	23.6 ± 2.68	5.5 ± 0.49	29.1 ± 2.37

V/3 M switch with 2-in.-diam electrodes, pulse charged to +980 kV

TABLE X

70, 40, 15	10.5 ± 0.93	8.8 ± 0.32	19.2 ± 1.12
85, 40, 15	13.2 ± 1.11	9.6 ± 0.33	22.8 ± 1.33
115, 40, 15	19.0 ± 2.51	8.9 ± 0.00	27.9 ± 2.62
135, 40, 15	28.0 ± 4.70	8.1 ± 0.92	36.1 ± 4.36

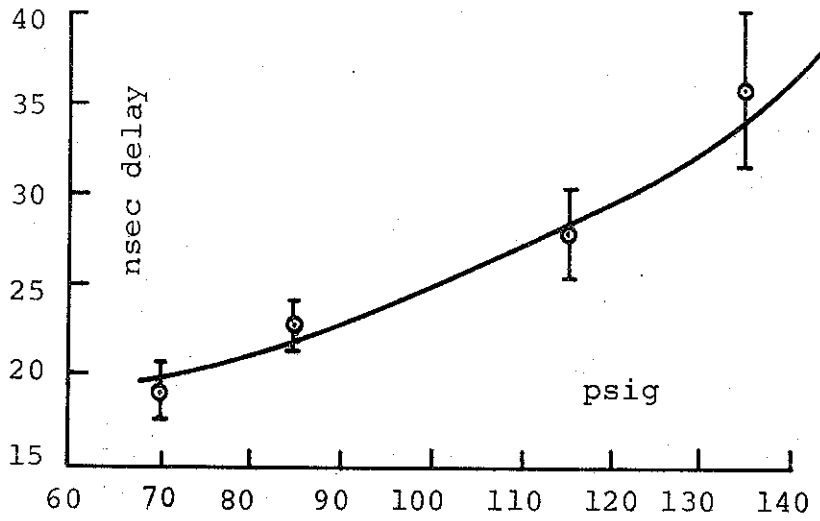
V/2 M switch with 3-in.-diam electrodes, pulse charged to +1.1 MV

TABLE XI

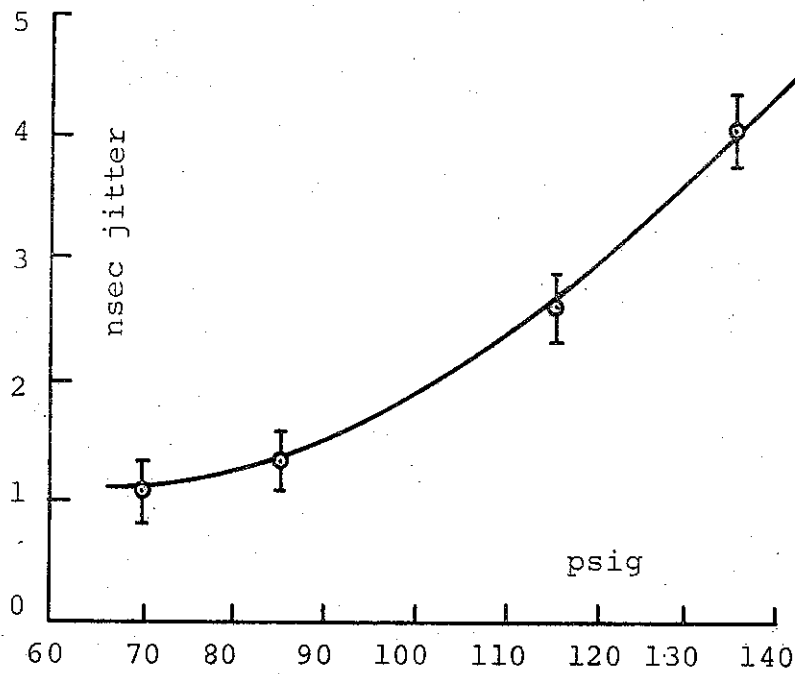
90, 40 ¹	8.8 ± 1.00	4.2 ± 1.57	13.0 ± 2.24
105, 40 ¹	9.8 ± 0.50	6.1 ± 0.33	15.9 ± 0.75
120, 40 ¹	11.1 ± 0.48	8.2 ± 1.19	19.3 ± 1.49
135, 40 ^{1,3}	7.9 ± 0.46	6.3 ± 1.05	15.2 ± 1.33
150, 40 ^{2,3}	7.0 ± 0.01	10.1 ± ----	17.1 ± ----
180, 40 ^{2,3}	9.4 ± 0.54	10.9 ± 4.21	18.3 ± 2.31

V/3 M switch 2-in.-diam electrodes with 40 pF cap in place of I-gap,
pulse charge equals -1.25 MV

- (1) Experimental error ± 0.25 nsec
- (2) Experimental error ± 0.40 nsec
- (3) Reflective inductance in trigger transmission line reduced.



a. Delay--Error Bars = \pm Jitter



b. Jitter--Error Bars = Measurement Error

FIGURE 38. OVERALL DELAY AND JITTER FOR V/2 M SWITCH
3-in. DIAM ELECTRODES. PULSE CHARGED TO +1.1 MV

In Figure 35 the voltage at which the S-gap breaks is plotted against pressure. Since the gap is symmetrical, no difference in polarity could be observed. The voltage finally applied to the middle electrode may be as much as $0.9 V_{tr}$, as explained in Section III, A, 4, Experimental Circuit.

Table XII is the first dealing with dependence on trigger voltage. Only the trigger changes. It is obvious that in this circuit the optimum trigger voltage is neither too high nor too low. If too low the jitter in the first part of the switch increases; if too high the jitter in the second part increases. This phenomenon is certainly due to the effect of the trigger pulse in reducing the voltage on the second half and is hence a property of the experiment. It is clear that the trigger amplitude is not critical.

The data in Table XIII was taken at a higher pressure, same voltage, and a slightly different M switch. The jitter at 55 psig on S was not computed since there was not enough data to get the measurement accurately

For the data in Table XIV, the V/2 switch was pulse-charged in the opposite polarity from which it was designed. The negative polarity causes a great deal of jitter to appear on the second part of the switch. In an attempt to decrease this jitter the trigger voltage was decreased, effecting a slight decrease in jitter.

4. Jitter Variation Near Self-Breakdown at Different Pressures

For a given M-switch in a given circuit, the behavior is determined by the voltage on the switch, the pressure in the switch, and the trigger voltage. While the effect of varying the latter

TABLE XII

M, S, I, (psig)	delay ₁ ± jitter ₁ (nsec)	delay ₂ ± jitter	delay _o ± jitter _o (overall)
90, 25, 15	11.4 ± 0.66	6.0 ± 0.76	17.3 ± 1.02
90, 40, 20	9.8 ± 0.44	5.2 ± 0.38	15.0 ± 0.76
90, 60, 35	9.7 ± 0.44	5.5 ± 0.49	-----

V/3 M switch with 2-in.-diam electrodes, pulse charged to -1.25 MV, experimental error ± 0.25 nsec

TABLE XIII

120, 30, 20	13.9 ± 1.02	7.3 ± 0.48	22.2 ± 1.52
120, 40, 20	12.4 ± 0.46	8.0 ± 0.40	20.4 ± 0.71
120, 55, 25	11.3-----	8.4-----	19.7-----

V/3 M switch with 3-in.-diam electrodes, pulse charged to -1.25 MV
(1) experimental error ± 0.26 nsec; (2) experimental error ± 0.40 nsec

TABLE XIV

70, 20, 15	10.3 ± 0.50	10.0 ± 0.95	20.3 ± 1.39
70, 40, 15	9.0 ± 0.24	11.5 ± 1.37	20.5 ± 1.50

V/2 M switch with 2-in.-diam electrodes, pulse charged to -1.1 MV
experimental error equals ± 0.25 nsec

TABLE XV

				(Overall Voltage)
70, 40, 15	9.9 ± 0.67	4.9 ± 0.49	14.8 ± 0.60	-1.1 MV
90, 40, 20	11.5 ± 0.45	6.5 ± 0.38	18.0 ± 0.57	-1.25MV

V/3 M switch with 3-in.-diam electrodes, experimental error ± 0.25 nsec

TABLE XVI

				(Trigger Impedance)
90, 40, 20	8.8 ± 0.32	8.2 ± 1.32	16.9 ± 1.53	0Ω
90, 40, 20	9.8 ± 0.44	5.2 ± 0.38	15.0 ± 0.76	120Ω

V/3 M switch with 2-in.-diam electrodes, -1.25 MV, experimental error ± 0.25 nsec

two has been demonstrated, it is still interesting to take the first two variables together and find the combinations that set the switch to roughly 80% of self-fire and then compare them. In Table XV, a $\approx 13\%$ increase in voltage and pressure causes a small decrease in jitter, but not quite enough to be significant. If the trigger voltage had been raised correspondingly there may have been a bigger difference.

5. Dependence on Trigger Circuit Parameters

Having found the optimum trigger voltage, it is of interest how best to transmit it to the middle electrode. Elimination of the $120\text{-}\Omega$ resistor (Figure 5) at the end of the transmission line would increase the amount of trigger available to fire the first part of the M switch, but after it had fired, voltage would be drained off more quickly from the charged electrode through the middle electrode and transmission-line to ground. Table XVI illustrates the effect of eliminating the $120\text{-}\Omega$ resistor. If the resistor were increased in value it would cause an increase in jitter in the first part of the switch and a decrease in the second. The optimum probably was reached with $120\text{-}\Omega$ because the two jitters are roughly equal.

To decrease the decay of voltage through the transmission line, a 40 pF capacitor was substituted for the I-gap. The jitter did not decrease in the second part, but generally increased (Table XVII). The balancing resistors were not sufficiently low to balance the additional capacity on the middle electrodes, causing the switch to perform poorly. The I-gap was put in series with the capacitor to counteract this effect and the lowest jitter of the entire experiment was observed. The jitter was below $1/2\text{ nsec}$ near self-breakdown; moreover, it was under 1 nsec to nearly 1.8 times self-breakdown pressure.

TABLE XVII

M,S,I	Delay ₁ ± jitter ₁	Delay ₂ ± jitter ₂	Delay ₀ ± jitter ₀	Trigger Line
90,40,20 ¹	11.5 ± 0.45	6.5 ± 0.38	18.0 ± 0.57	I-gap
90,40 ¹	8.8 ± 1.00	4.2 ± 1.57	13.0 ± 2.24	40 pF Cap
90,40,20 ¹	8.2 ± 0.29	4.7 ± 0	13.0 ± 0.39	I-gap & Cap
120,40,20 ¹	12.4 ± 0.46	8.0 ± 0.40	20.4 ± 0.71	I-gap
120,40 ¹	11.1 ± 0.48	8.2 ± 1.19	19.3 ± 1.49	40 pF Cap
180,40,20 ¹	13.3 ± 0.35	9.5 ± 4.25	22.7 ± 3.82	I-gap
180, 40 ²	9.4 ± 54	10.9 ± 4.21	18.3 ± 2.31	40 pF Cap
180,40,15 ²	10.4 ± 0	6.3 ± 0.39	10.7 ± 0.66	I-gap & Cap

V/3 M switch with 3-in.-diam electrodes, -1.25 MV

(1) experimental error ± 0.25 nsec

(2) experimental error ± 0.40 nsec

6. The Effect of the Impedance Driving M-Switch

The only values of resistors that were tried between the 250 pF capacitor and the M-switch were 240 ohms, 80 ohms, and 5 to 10 ohms. Jitters under 1 nsec were observed with the last two but in the 240 ohm case, the jitter greatly increased. The only problem is that a very low impedance caused the absence of damping, which allowed high-frequency ringing and made it more difficult to read signals. There was no determination of how high the impedance could be and still achieve subnanosecond jitter, but it was felt that it would be around 150 ohms. At that point the RC time to recharge the M-switch is 3 nsec, slower than the discharge through the trigger line.

7. Polarity Effects

It was found that V/3 M-switches worked considerably better when the overall voltage was negative (Table XVIII), although if considerable care were taken it was possible to achieve \approx 1-nsec jitter with positive polarity at M pressures near self-breakdown. The V/2 switch was the other way round, working much better with a positive overall voltage (Table XIX).

Since it is easier to breakdown a positive point to plane than a negative one in SF₆, one expected the main source of jitter would be in the part of the switching sequence when the middle electrode would be negative. The first event, switching the middle electrode to the HV side, was the main source of jitter with positive overall voltage. The V/3 switch was offset to minimize jitter in the second part when the overall voltage was negative.

TABLE XVIII

M,S,I	Delay ₁ ± jitter ₁	Delay ₂ ± jitter ₂	Delay ₀ ± jitter ₀	Overall Voltage
70,40,15	9.9 ± 0.67	4.9 ± 0.49	14.8 ± 0.60	-1.1 MV
70,40,15	13.4 ± 0.74	4.6 ± 0.29	17.9 ± 0.80	+1.1 MV

V/3 M switch with 3-in.-diam electrodes, ±0.25 nsec

TABLE XIX

M,S,I	Delay ₁ ± jitter ₁	Delay ₂ ± jitter ₂	Delay ₀ ± jitter ₀	Overall Voltage
70,40,15	9.0 ± 0.24	11.5 ± 1.37	20.5 ± 1.50	-1.1 MV
70,40,15	13.5 ± 0.93	8.8 ± 0.32	19.2 ± 1.12	+1.1 MV

V/2 M switch with 3-in.-diam electrodes, ±0.25 nsec

It was expected the V/2 M switch would perform better in the first part of switching than the V/3 switch because the first gap to fire was smaller. Unfortunately, this result was clear only at pressures considerably above self-breakdown pressure. At lower pressures the V/3 seemed to perform better. Further investigation was indicated but time did not permit it.

A different type of V/2 M-switch was tested earlier that used a wire down the center of the gap rather than the sharp-edged plane. The jitter was approximately the same as the other V/2 switch.

8. Miscellaneous Sources of Jitter

Miscellaneous sources of jitter become significant when the overall jitter is less than 1/2 nanosecond.

a. Trigger Amplitude Variation

Even though the pressure in the S gap was kept constant in each series of shots, the trigger voltage typically had a 3 to 5% fractional deviation. A 4% trigger voltage deviation would be expected to give rise to $\approx 1\text{-}1/2\%$ fractional deviation jitter in firing the first part of a V/3 M switch negatively charged. This was calculated from the dependence of the breakdown time of the first half of M on S pressure (shown in Table XIII), assuming S pressure proportional to S voltage. As an example, the linear correlation coefficient, S vs first-part delay, was calculated for the V/3 M switch with 2-in.-diam electrodes at -1.25 MV pressurized to M 90, S 40, I 20.

The correlation between trigger amplitude and first-part delay was -0.36. The fractional deviation of trigger voltage was 4% and the first-part delay (13 nsec) deviated 3 1/2% (0.5 nsec). Note that $(0.36) \times (3\text{-}1/2\%) = \approx 1\%$ roughly what would be expected due

to trigger pulse variation. Thus in this example the real fractional deviation (jitter) is only 3% (≈ 0.4 nsec) in the M-switch when the contribution due to S jitter is taken out. The effect becomes less and less important as the switch is pressurized and the M jitter rises, and more important as M jitter decreases. When triggering many M switches with a single trigger pulse there can be no trigger pulse deviation switch-to-switch, and, hence, a slight decrease in overall jitter would be obtained.

b. I-Gap Jitter

The I-gap jitter will remain, even in multiple switching, as long as an I gap is used for each M switch. A typical set of data shows it to be too small to be accurately measured, $\approx 1/3$ nsec $\pm 1/4$ nsec. Since the jitter is independent of M jitter the true overall jitter can be predicted by adding the square of I jitter to the square of M jitter and taking the square root of the sum.

c. Photographic Random Error

Although the I-gap jitter was distinct and clearly separate from the overall jitter the pseudo jitter due to random error in reading oscilloscope photos had to be mathematically eliminated from the table. The random error in 10-nsec traces was ± 0.4 nsec and in the 5-nsec trace was ± 0.25 nsec. The square of these errors was subtracted from the square of the measured jitter and the square root of the difference was presented.

9. Conclusions

The three-electrode SF₆ switches tested all have shown a high degree of reliability in addition to their low jitter, prompt switching characteristics. Subnanosecond jitters have been achieved at voltages up to -1.25 MV with a V/3 M switch, while ≈ 1 nsec jitters at + 1.1 MV were produced with a V/2 switch. Neither switch

was entirely satisfactory at the opposite polarity for which they were intended, although reasonably low jitters could be obtained by very careful adjustment of the pressure of M-switch for the overall voltage.

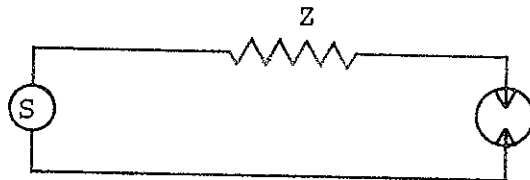
Further improvements in the jitter of the M-switch may come from improving the trigger circuit. A large step in this direction was made by combining the I gap and a 40-pF series capacitor that gave the lowest jitters of the experiment. In fact, for any application of the M-switch, it is essential to consider the trigger circuit as equally important for optimum performance.

SECTION IV

EARLY RESISTIVE PHASE MEASUREMENTS

The apparatus described in Section III was used for a brief and preliminary study of the pulse shapes produced by a self-closing gas switch in a constant-impedance transmission line. The trigger waveform of the previous experiments was recorded using the E-field probe at a range of S-switch pressures, filling that gap variously with SF₆, Freon 12, and nitrogen. The trigger line was an open circuit. The objective was to observe the early resistive phase of the gas spark; that is, that time in which the impedance of the ionized channel is greater than the impedance the spark is driving, but small enough to produce a noticeable voltage change in the source. Current flow is small compared with the eventual short-circuit current of the source, but nevertheless quite significant.

A. RISETIME PARAMETERS



The principal risetimes produced by a switch in the circuit shown are the inductive and resistive phases. The inductive risetime is simply L/Z where L is the inductance of the switch; if the resistance of the switch is assumed to change from infinity to zero at $t = 0$, the current can be subsequently described by the equation $i = V/Z (1 - e^{-t/\tau_L})$, where $\tau_L = L/Z$. τ_L is an "e-folding" risetime, and di/dt is a maximum at $t = 0$. The concept of resistive phase originated with J. C. Martin (AWRE, Aldermaston, U.K.) who showed that the expression

$$\tau_R = \frac{5\rho^{1/2}}{Z^{1/3}F^{4/3}}$$

closely approximated the behavior in liquids, solids, and gases. The resistive phase τ_R is thought of as the time when the spark impedance is comparable to that of the source. τ_R can be measured as $\frac{i_{\max}}{(di/dt)_{\max}}$, or for the pulse generated (in a transmission line for example) V/V_{\max} . This would be the same as the e-folding time in the inductive example, but in this case di/dt is not a maximum when $i = 0$. τ_R is a description of what is usually the most significant portion of the pulse rise, the portion of greatest slope.

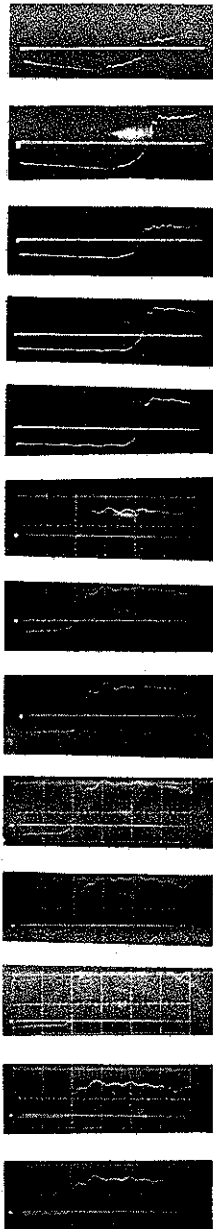
The time of greatest slope may be preceded by a period when the channel is forming and heating, during which the impedance is much higher than Z , but this period is often unimportant because little current flows. It has been observed however that when SF_6 switches drove relatively high impedances ($\approx 100 \Omega$), the early high resistance phase was often quite prolonged and led to considerable degradation of the pulse rise. The effect was observed both in uniform field switches (ARES I Quarter Scale Study) and edge plane switches (SIEGE II Phase II study). The purpose of the experiments performed here was to investigate more fully the effect of gas identity and pressure.

B. RESULTS

1. Experimental Techniques

Figure 27 shows the switch used in the tests. The electrode spacing was 1.5 cm and the electrodes were of tungsten alloy.

Figure 39 shows a typical series of waveforms measured in the 90-ohm trigger line with successively increasing SF_6 pressures in the main switch. Of course, the switching voltage increased with pressure. Wave shape varies from shot to shot, and this accounts for some of the variation in the Figure 39. The trend to sharper rising waveforms at higher pressures is clear however.



0 psig, 10 nsec/cm, 5:1 Attenuation
10 psig, 10 nsec/cm, 5:1 Attenuation
20 psig, 10 nsec/cm, 10:1 Attenuation
25 psig, 10 nsec/cm, 10:1 Attenuation
30 psig, 10 nsec/cm, 10:1 Attenuation
30 psig, 5 nsec/cm, 9:1 Attenuation
40 psig, 5 nsec/cm, 10:1 Attenuation
50 psig, 5 nsec/cm, 10:1 Attenuation
60 psig, 5 nsec/cm, 10:1 Attenuation
70 psig, 5 nsec/cm, 10:1 Attenuation
80 psig, 5 nsec/cm, 10:1 Attenuation
90 psig, 5 nsec/cm, 18:1 Attenuation
100 psig, 5 nsec/cm, 18:1 Attenuation

FIGURE 39. RESISTIVE PHASE OF TRIGGER PULSE

To present the results numerically, it was necessary to define various new wave-shape parameters, which is made somewhat difficult because of the variation in shape. Typical shapes are sketched in Figure 40 where it is seen that the two parameters used are, like τ_R , linked to the point of greatest slope. The early resistive (or "fizzle") phase is defined as the interval between the time when the first current flows and the time when $\frac{di}{dt}$ or V is greatest. The onset of current is sometimes sharp (Figure 40) and sometimes indistinct (Figure 40b) and the current increases slowly until a value is reached at which a relatively distinct break occurs and the rise rate rapidly attains its maximum. The current at which this break occurs is denoted by i_b . Sometimes two breaks can be seen (as in Figure 40c). Also seen in Figure 40 is the total risetime.

Most measurements were performed using SF_6 at up to 100 psig. Freon 12 was tested up to 60 psig. (It liquified at 67 psig at room temperature.)

Figure 41 shows that τ_F was a strong function of pressure. τ_F had a standard deviation of 10 to 20%.

Figure 42a shows the current at which the break, or steep rise, occurred. This by comparison was almost independent of pressure at about 1000 amps in SF_6 . It varied shot to shot by as much as a factor of 2, and at the highest pressures the early resistive phase could not be clearly identified on some shots. Variation did not seem to be correlated with the breakdown voltage, which was also subject to a small scatter. There may have been a slight tendency for τ_F to decrease on successive shots when the gas in the switch was not changed, but this is very uncertain.

While the value of i_b remains little changed as pressure increases, the peak pulse current in the fixed impedance rises

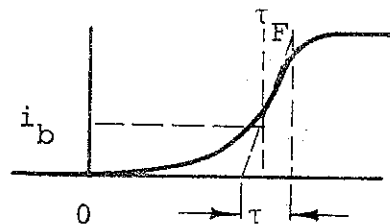
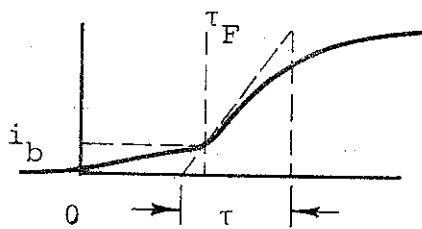
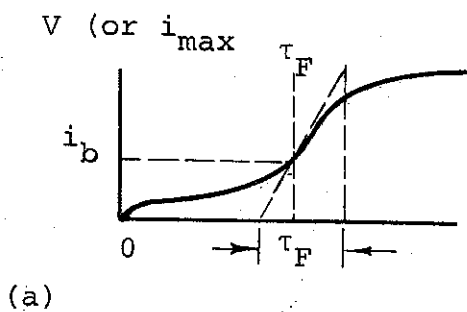


FIGURE 40. EARLY RESISTIVE PHASE AND VOLTAGE RISE TIME

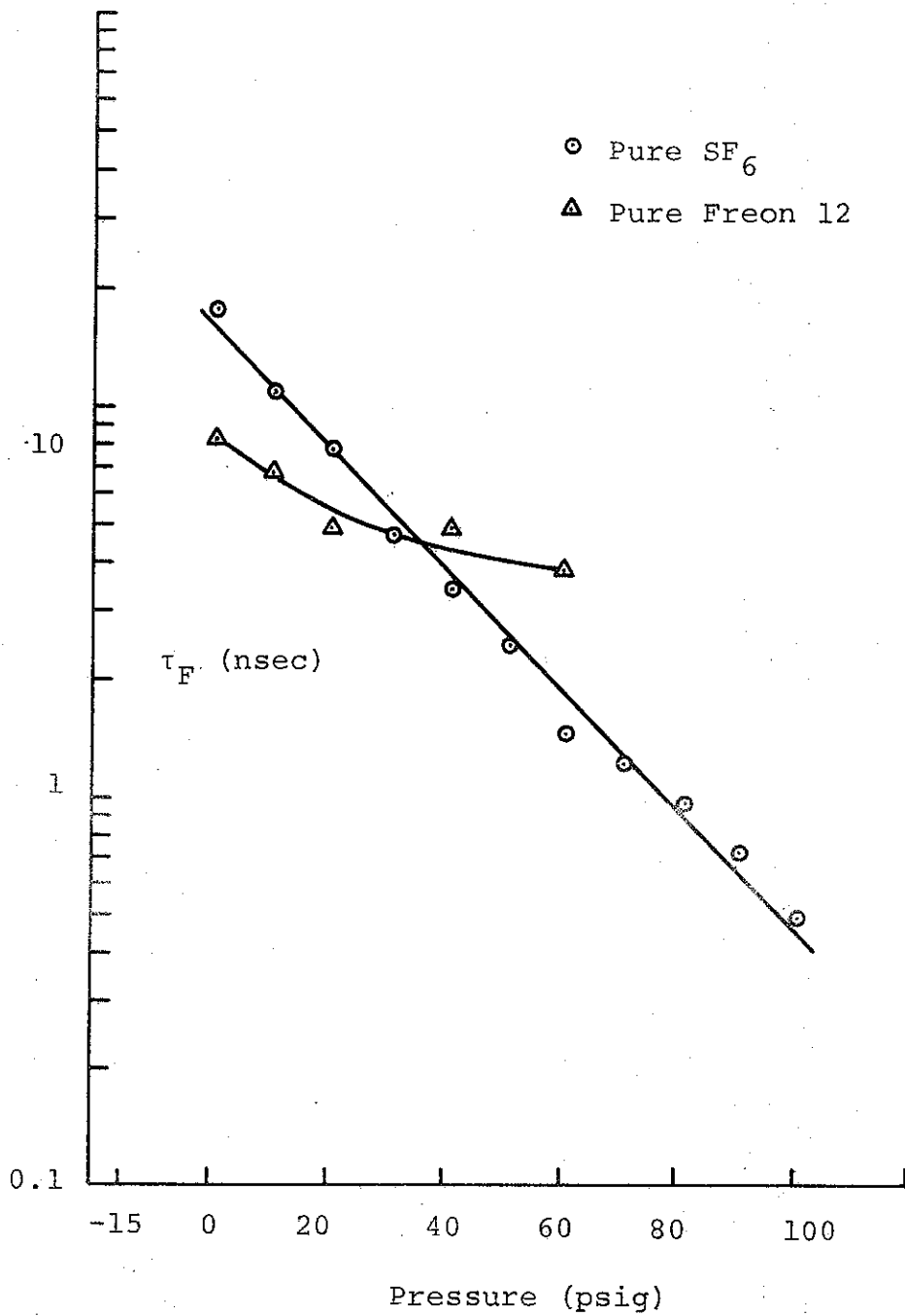


FIGURE 41. EARLY RESISTIVE (FIZZLE) PHASE VERSUS PRESSURE

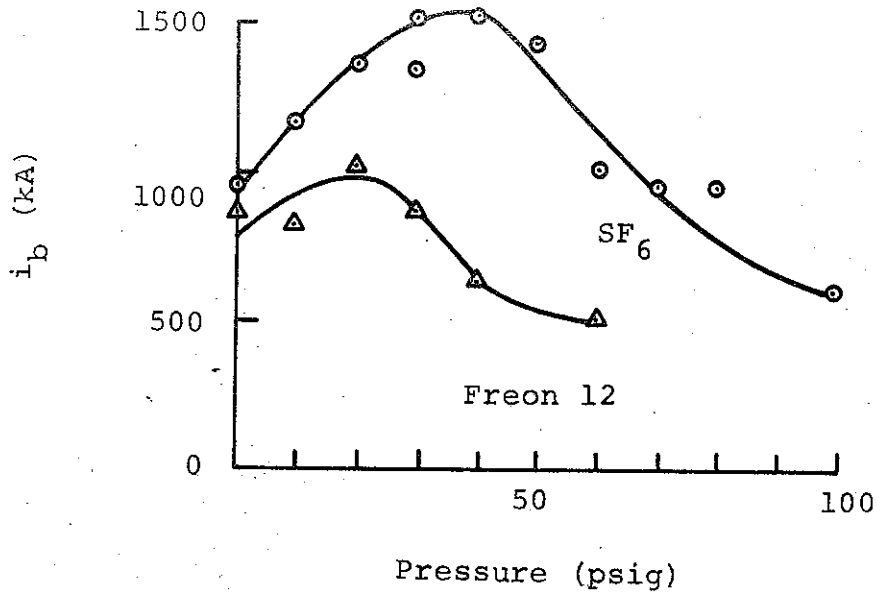


FIGURE 42a. CURRENT AT WHICH $(V)_{max}$ IS OBSERVED

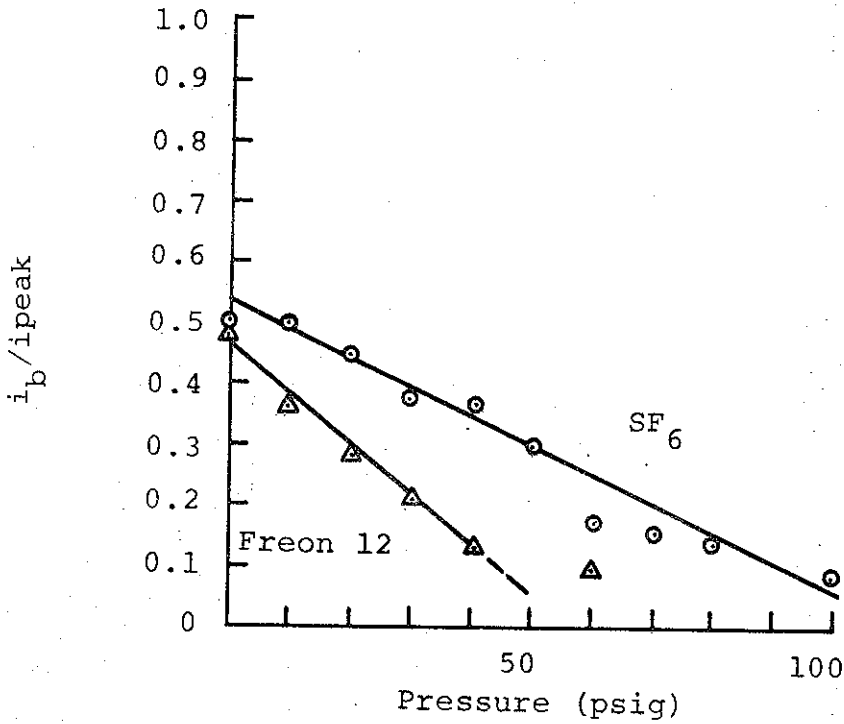


FIGURE 42b. FRACTION OF VOLTAGE OR CURRENT RISE AT WHICH $(V)_{max}$ IS OBSERVED

8309

steadily so that the early resistive phase affects a smaller fraction of the total pulse amplitude (see Figure 42).

The results for Freon 12 are also shown. Freon 12 has a closely similar breakdown field, but its density relative to air is about 5 compared with about 6 for SF₆. In general, Freon gave a better pulse shape; above 30 psig the early resistive effect was so small as to be hard to distinguish against a ripple on the waveform. Freon, however, has the disadvantages of being limited to pressures of about 60 psig or less, as well as producing undesirable compounds on decomposition--in some cases free carbon.

Figure 43 shows the risetime, τ , measured from the portion of greatest slope, as a function of pressure. The calculated value of τ_R (from the observed values of F and calculated ρ in each case) is also shown. The general agreement in the variation with pressure is good. The differences are probably attributable to τ_L (0.6 nsec) and the risetime of the monitoring system (cable 1/2 nsec; scope, 0.1 nsec; attenuators, 1/4 nsec) which are almost constant. In view of the different characteristics of the various component risetimes, no more quantitative comparison by risetime addition or subtraction is possible.

An apparently anomalous result was obtained at 0 psig of Freon. At this point, however, the rapid portion of the rise occurred only after the current had already risen more slowly to half its final value.

Experiments were also conducted with nitrogen, but these were at the end of the program and were constrained to be brief. Pressures of 0.25, and 100 psig were used; the results are given in Table XX. At 0 and 25 no early resistive phase could be distinguished at all. The rate of rise of the pulse appeared to

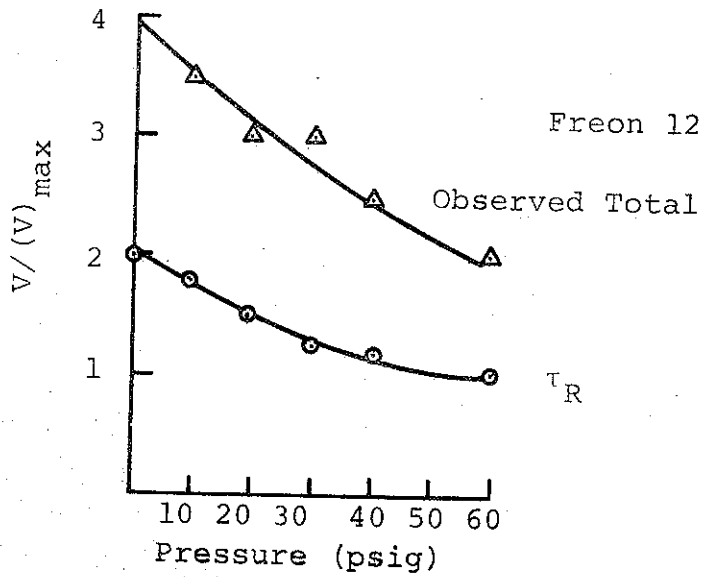
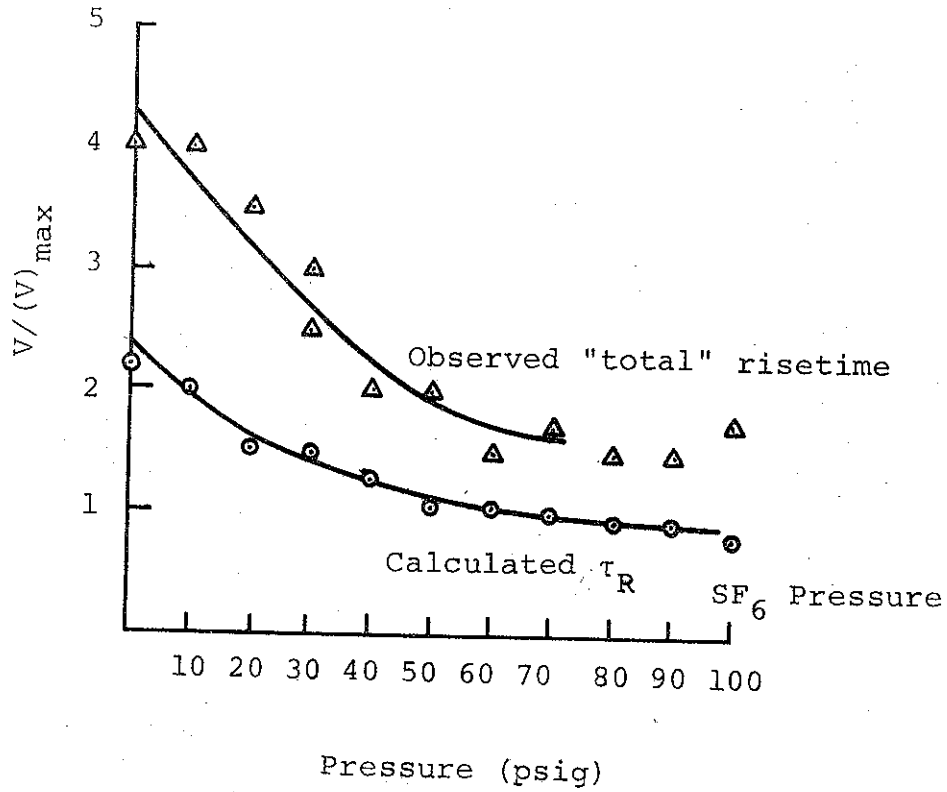


FIGURE 43. RISE TIME OF SF₆ SWITCH INTO 90Ω

attain maximum value immediately, and was preceded by a current of less than about 75 amps.

At 0 psi, the switch is driven well over the dc breakdown strength of N_2 (about 25 kV/cm) because the applied voltage rises rapidly and the low field is unable to extract initiating electrons from the electrodes; the rising waveform approximated an exponential.

At 25 psig the waveform was close to a linear ramp, and the risetime τ was 4-1/2 nsec, where about 2-1/2 nsec would have been expected on the basis of a calculated resistive phase of 1 to 2 nsec and comparing with the other results to estimate the effect of adding the other risetime components. At 100 psig, an early resistive phase could be distinguished for the first time and the ensuing risetime was consistent with a resistive phase of less than 1 nsec.

At both 25 and at 100 psig the waveshape with N_2 (Table XX) was much cleaner than would be expected in SF_6 either at a corresponding density (-8 psig and 5 psig, respectively) or at a corresponding field (-3 psig and 20 psig, respectively). At 100 psi, i_b was only 200 amps compared to about 1000 amps in Freon or SF_6 and N_2 might be a much better switch medium than pure SF_6 .

2. Effect of Gap Spacing, Impedance, and Field

Time did not permit variations of either of these parameters. In most cases, the early resistive phase drives only a small fraction of the short circuit current of the source, so that the current time history would probably not be a strong function of the driving impedance. For lower impedances, the same early time currents produce less effect in the circuit; after the breaking point, the usual resistive phase formula can be applied. For higher impedances

TABLE XX

RISETIME MEASUREMENTS USING N₂

<u>Pressure (psig)</u>	<u>V (MV)</u>	<u>F (MV/cm)</u>	<u>τ_F</u>	<u>i_b (amp)</u>	<u>τ</u>	<u>τ_R</u>
0	0.085	0.05	none	< 75	2½	1.4
25	0.13	0.08	none	< 75	4½	1.2
100	0.215	0.17	5½	200	1½	0.7

the effect will be more noticeable, and it may be that smaller currents flowing at the beginning of τ_F would constitute a measurable effect over a longer period. This is especially possible in cases when the onset of current in the tests described has not been found to be sudden.

If the electrode spacing is increased at fixed pressure and impedance, the driving voltage and hence the peak current increase, suggesting that the early current again is less important.

One general scaling law can be postulated: that if gap spacing and impedance are changed in the same ratio at a fixed pressure so that the peak current is unchanged, the waveform will be invariant. If the length of the spark is doubled, for example, the breakdown voltage will double and if the driving impedance also doubles, each half will have the same current-voltage-time history as before. This assumes that the spark is uniform along its length; however, and this may not be the case, especially if branching occurs.

Finally, while the above arguments may be cautiously applied to uniform field gaps in which the breakdown field is only a function of pressure, introduction of sharp edges to convert the gap to a point plane switch (thus achieving greater reproducibility) can achieve a whole range of fields at any given pressure as can triggering the gap with a third electrode. The effect of the field as an independent variable cannot be estimated on the basis of the experiments performed so far. Correlation with the point-plane gaps tested in the SIEGE II contract is almost impossible because other parameters (spacing, driving impedance) also differ.

3. Conclusions

During the breakdown of Freon 12 and SF₆ the current rises comparatively slowly until a value of about 1000 amps is reached. The time taken is called the early resistive phase, and falls exponentially with increasing pressure. For a 1.7 cm uniform field spark driving 1000 Ω, the duration is about 10 nsec at 0 psig and about 1 nsec at 100 psig. Considerable waveshape distortion can arise below about 20 psig. The effect may be greatest for small gaps and high-circuit impedances. The effect of changing the average breakdown field by local enhancement is unknown. Nitrogen at corresponding densities and fields yields much superior waveforms, and mixtures of SF₆ and N₂ may be advantageous.

